

REMARKS

Claims 1-5, 7-11 and 14-17 were rejected under 35 U.S.C. § 103(a) as being unpatentable over U.S. Patent 6,150,426 to Curtin et al in view of U.S. Patent 3,085,083 to Schreyer. Further, claims 1-17 stand rejected under 35 U.S.C. § 103(a) as being unpatentable over WO 2004/018527 to Tatemoto et al (with citation to U.S. 2005/0228127 A1) in view of Schreyer. The grounds for rejection remain the same as set forth in the previous Office Action.

Applicants have carefully considered the Examiner's Response to Arguments as set forth at pages 8-12 of the Office Action, and submit two technical literature references in response, discussed below. Moreover, Applicants reiterate that the present claims are patentable for the same reasons set forth in the Response filed February 26, 2009 when considered in view of the subject two technical literature references.

Response to Claim Rejections:

The fluoropolymer of present claim 1 contains acid/acid salt groups and has -CF₂H groups at polymer chain terminals.

The fluoropolymer of claim 1 is stable and is particularly suitable for use in the field of solid polymer electrolyte fuel cells and in other fields where stability is required. See page 27, lines 11-14 of the specification.

The result of stability testing using Fenton's reagent reveals the effect of the invention. See page 25, lines 17-21 and page 27, lines 5-8 of the specification.

Investigators in the field of polymers containing acid/acid salt groups believe that -CF₂H group is an unstable functional group resulting in the problem of gradual polymer decomposition. The state of the art is disclosed in paragraph [0004] of U.S. 2006/063903 and paragraph [0018] of U.S. 2006/0287497.

Paragraph [0004] of U.S. 2006/0063903 A1 is reproduced below:

However, a perfluorinated polymer having sulfonic groups to be used as a polymer contained in a membrane and an electrode usually has unstable functional groups such as -COOH groups, -CF=CF₂ groups, -COF groups and -CF₂H groups at some molecular chain terminals, and therefore, there was such a problem that a polymer gradually decomposes during long-term fuel cell operations, followed by decreasing the power generation voltage. In addition, there was such a problem that the fuel cell operation cannot be conducted because decrease of the mechanical strength due to the polymer decomposition, locally causes pinholes, breaking, abrasion or the like.

Paragraph [0018] of U.S. 2006/0287497 is reproduced below:

The present inventors considered that since a linear perfluoropolymer having sulfonic acid groups which has been commonly used for fuel cells, has unstable functional groups such as -COOH groups, -CF=CF₂ groups, -COF groups and -CF₂H groups at same molecular chain terminals, such a polymer gradually decomposes during long-term operation when used for an electrolyte material for polymer electrolyte fuel cells, whereby the power generation voltage decreases and the membrane strength decreases to locally cause pinholes, breaking, abrasion or the like, and they have found that the durability can be greatly improved by fluorinating (contacting with fluorine gas) such a polymer so as to stabilize the molecule terminals by perfluorination. However, in a case where the polymer was exposed to severe operation conditions, such durability was not good enough. Accordingly, they have conducted a further study for improvement of the durability, and as a result, have found that the durability can be remarkably improved by fluorinating a polymer having alicyclic structures in its main chain and further having sulfonic acid groups, as compared with the durability improved by fluorinating the conventional polymer.

However, contrary to the conventional belief of investigators in this field of art, the present inventors found that the fluoropolymer of claim 1 containing acid/acid salt groups and having -CF₂H groups at polymer chain terminals tolerates Fenton's reagent (i.e., OH radicals) to thereby achieve the present invention.

Turning to the cited prior art, Curtin et al and Tatemoto et al, primarily relied upon in the above two prior art rejections, disclose no polymer-containing acid/acid salt groups and having -CF₂H groups at polymer chain terminals as required by present claim 1.

Schreyer does not disclose that polymers having $-\text{CF}_2\text{H}$ groups have resistance to OH radicals. Schreyer only teaches thermal stability of copolymers having no acid/acid salt groups. See col. 1, lines 70-71.

Therefore, there is no teaching or suggestion in the cited prior art which would lead one of ordinary skill to modify the fluoropolymers of Curtin et al or Tatemoto et al (having an acid/acid salt group) with the endgroups taught by Schreyer (disclosing fluorocarbon polymers having no acid/acid salt groups).

For the above reasons, it is respectfully submitted that the present claims are patentable over the cited prior art, and withdrawal of the foregoing rejections under 35 U.S.C. § 103(a) is respectfully requested.

Applicants' Answer to the Examiner's Response to Arguments:

(1) Additional Documents

In paragraph 40 of the Office Action, the Examiner states "Both Curtin and Tatemoto teach fluoropolymers, therefore the process of Schreyer could be used with Curtin and Tatemoto."

The fluoropolymer with SO_3M group must be resistant to OH radical.

Curtin et al, *Advanced Materials for Improved PEMFC Performance and Life*, Journal of Power Sources 131 (2004) 41-48 (copy attached) discloses that OH radical attacks any H-containing terminal bonds present in the polymer. See page 42, right-hand column, lines 20-30. H-containing terminal bonds are included in such end groups as disclosed in Pianca et al, *Endgroups in Fluoropolymers*, Journal of Fluorine Chemistry 95 (1999) 71-84. See page 72, left-hand column, lines 19-25.

CF₂H group is clearly unstable in the field of Curtin. Therefore, a person skilled in this field of art would not combine the applied references. This is because Curtin teaches a fluoropolymer having SO₃M group.

(2) Schreyer

The Examiner further states that “these references contradict the statements of Schreyer regarding the stability of -CF₂H endgroups” (paragraph 43), and that “the references cited by the Applicant only give a list of several functional groups, with no mechanistic information of the stability or decomposition” (paragraph 48).

However, there is no conflict.

U.S. 2006/0063903 and U.S. 2006/0287497 teach that CF₂H endgroup is unstable against OH radical. The additional references give mechanistic information on the stability or decomposition.

In contrast, Schreyer teaches that -CF₂H endgroup is thermally stable.

The Examiner also states that “one of ordinary skill in the art would recognize that stability is a relative term” (paragraph 49).

That is true. -CF₃ group is stable and -CF₂H and -COOH groups are unstable against OH radical at the time the invention was made.

Since different stabilities might be necessary for different applications as the Examiner states in paragraph 49, a skilled artisan would select -CF₃ group to improve the stability of a polymer with SO₃H group.

The Examiner further states “U.S. 2006/0063903 states that conversion of -COOH to -CF₂H has been proposed to stabilize the chain terminals” (paragraph 50).

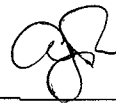
However, the subject passage cites U.S. Patent 3,085,083 to Schreyer which does not disclose that polymers having $-CF_2H$ groups have resistance to OH radicals and which only teaches thermal stability of copolymers having no acid/acid salt groups. U.S. 2006/0063903 does not suggest that CF_2H is useful as an endgroup, but rather that $-CF_3$ is required for a polymer with SO_3H group. See [0033] of U.S. 2006/0063903.

Withdrawal of all rejections and allowance of claims 1-17 is earnestly solicited.

In the event that the Examiner believes that it may be helpful to advance the prosecution of this application, the Examiner is invited to contact the undersigned at the local Washington, D.C. telephone number indicated below.

The USPTO is directed and authorized to charge all required fees, except for the Issue Fee and the Publication Fee, to Deposit Account No. 19-4880. Please also credit any overpayments to said Deposit Account.

Respectfully submitted,



Abraham J. Rosner
Registration No. 33,276

SUGHRUE MION, PLLC
Telephone: (202) 293-7060
Facsimile: (202) 293-7860

WASHINGTON OFFICE

23373

CUSTOMER NUMBER

Date: July 15, 2009

Advanced materials for improved PEMFC performance and life

Dennis E. Curtin*, Robert D. Lousenberg, Timothy J. Henry,

Paul C. Tangeman, Monica E. Tisack

DuPont Fuel Cells, 22828 NC Highway 87 W, Fayetteville, NC, USA

Abstract

Physical and functional attributes are reviewed for recently developed Nafion® products that satisfy emerging fuel cell requirements—including stronger, more durable membranes, and polymer dispersions of higher quality and consistency for catalyst inks and film formation. Size exclusion chromatography (SEC) analysis has confirmed that dispersion viscosity is related to an “apparent” molar mass, resulting from a molecular aggregate structure. Membranes produced with solution-casting and advanced extrusion technologies exhibit improved water management and mechanical durability features, respectively. Additionally, DuPont has shown that experimentally modified Nafion® polymer exhibits 56% reduction in fluoride ion generation, which is considered a measure of membrane lifetime.
© 2004 Elsevier B.V. All rights reserved.

Keywords: Nafion®; Proton exchange membrane; Polymer dispersion; Fuel cell

1. Introduction

1.1. Nafion® PFSA polymer

DuPont introduced Nafion® perfluorinated polymer [1] in the mid-1960s. Nafion® is a copolymer of tetrafluoroethylene or “TFE”, and perfluoro(4-methyl-3,6-dioxo-7-octene-1-sulfonyl fluoride) or “vinyl ether”, as shown in Fig. 1. Nafion® polymer is a thermoplastic resin that can be melt-formed into typical shapes such as beads, film, and tubing. The perfluorinated composition of the copolymer imparts chemical and thermal stability rarely available with non-fluorinated polymers. The ionic functionality is introduced when the pendant sulfonyl fluoride groups (SO_2F) are chemically converted to sulfonic acid (SO_3H). The copolymer’s acid capacity is related to the relative amounts of co-monomers specified during polymerization, and can range from 0.67 to 1.25 meq. g^{-1} (1500–800EW, respectively).

The unique functional properties of Nafion® PFSA polymer have enabled a broad range of applications. Initially, Nafion® membranes were used for spacecraft fuel cells; however, by the early-1980s, membrane electrolysis production of chlorine and sodium hydroxide from sodium chloride emerged as the largest application for Nafion® membranes. Other important industrial applications include production

of high purity oxygen and hydrogen, recovery of precious metals, and dehydration/hydration of gas streams. In addition, Nafion® super-acid catalysts are used to produce fine chemicals. Starting in 1995, DuPont began a series of process and product development programs specific to PEM fuel cell applications.

1.2. Nafion® PFSA membranes

The traditional extrusion-cast membrane manufacturing process was developed for “thick” films, typically greater than 125 μm . The extruded polymer film must be converted from the SO_2F to the SO_3K form using an aqueous solution of potassium hydroxide and dimethyl sulfoxide, followed by an acid exchange with nitric acid to the final SO_3H form [2].

Technical advances in fuel cell design and performance have increased demand for thin membranes produced at production rates that will meet the lower conversion cost goals required for fuel cell applications. Furthermore, there is a growing demand for larger production lot sizes, increased roll lengths and improved physical appearance. To meet this need, DuPont developed a solution-casting process for supplying high-volume, low-cost membrane to the fuel cell industry that was planning automated processes for membrane electrode assemblies [3,4].

DuPont’s new membrane process uses typical solution-casting technology and equipment, as shown in Fig. 2. A base film [1] is unwound and measured for thickness [2].

* Corresponding author. Tel.: +1-910-678-1224; fax: +1-910-678-1496.
E-mail address: dennis.e.curtin@usa.dupont.com (D.E. Curtin).

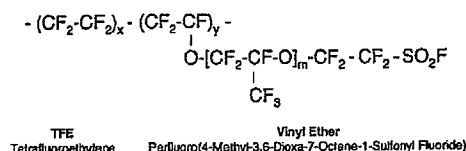


Fig. 1 Nafion® polymer structure before conversion to the sulfonic acid form.

Polymer dispersion is applied [3] to the base film, and both materials enter a dryer section [4]. The composite membrane/backing film is measured for total thickness [5], with the membrane thickness the difference from the initial backing film measurement. The membrane is inspected for defects [6], protected with a coversheet [7], and wound on a master roll [8]. The membrane is produced in a clean room environment [9]. Master rolls are slit into product rolls, which are individually sealed and packaged for shipment.

This process has several key advantages: (1) pre-qualification of large dispersion batches for quality (e.g., free of contamination) and expected performance (e.g., acid capacity); (2) increased overall production rates for H⁺ membrane from solution-casting as compared to polymer extrusion followed by chemical treatment; and (3) improved thickness control and uniformity, including the production capability of very thin membranes (e.g., 12.7 µm).

1.3 Nafion® PFSA polymer dispersions

Two patented high-pressure processes, solvent-based [5] and water-based [6], are used to convert Nafion® polymer (sulfonic acid form) into polymer dispersions having solids contents ranging from 5 to 20% by weight. These dispersions are formulated into carbon inks and catalyst coatings, and used either “as supplied” or with modifiers [7], and/or reinforcement materials to fabricate electrode coatings and membranes [8–10].

The manufacture of polymer dispersions has undergone considerable change since first introduced by DuPont, with the recent “second generation” dispersions exhibiting more stable and consistent viscosity, improved acid capacity and reduced metal ion content. These features enable more

predictable coating formulations, consistent processing, and improved fuel cell performance. A “third generation” dispersion is in the final R&D stages, and will provide broader formulation capabilities for both solvent and polymer content. It will also allow further process simplification for preparing coatings, casting membranes and fabrication of membrane electrode assemblies.

1.4. Polymer chemical stability

The useful lifetime of a membrane is related to the chemical stability of the ionomer. While Nafion® PFSA polymer has demonstrated highly efficient and stable performance in fuel cell applications, evidence of membrane thinning and fluoride ion detection in the product water indicates that the polymer is undergoing chemical attack. The fluoride loss rate is considered an excellent measure of the health and life expectancy of the membrane [11]. Peroxide radical attack on polymer endgroups [12] with residual H-containing terminal bonds is generally believed to be the principal degradation mechanism.

In this degradation mechanism, cross-over oxygen from the cathode side, or air bleed on the anode side, provides the oxygen needed to react with hydrogen from the anode side and produce H₂O₂, which can decompose to give •OH or •OOH radicals. These radicals can then attack any H-containing terminal bonds present in the polymer. Peroxide radical attack on H-containing endgroups is generally believed to be the principal degradation mechanism. This form of chemical attack is most aggressive in the presence of peroxide radicals at low relative humidity conditions and temperatures exceeding 90 °C.

Hydroxy or peroxy radicals resulting from the decomposition of hydrogen peroxide in the fuel cell attack the polymer at the endgroup sites and initiate decomposition. The reactive endgroups can be formed during the polymer manufacturing process and may be present in the polymer in small quantities. An example of attack on an endgroup such as CF₂X, where X = COOH, is shown below.

Several proposed mechanisms include the following sequential reactions: abstraction of hydrogen from an acid endgroup to give a perfluorocarbon radical, carbon dioxide and water (step 1). The perfluorocarbon radical can react with hydroxy radical to form an intermediate that rearranges to an acid fluoride and one equivalent of hydrogen fluoride (step 2). Hydrolysis of the acid fluoride generates a second equivalent of HF and another acid endgroup (step 3).

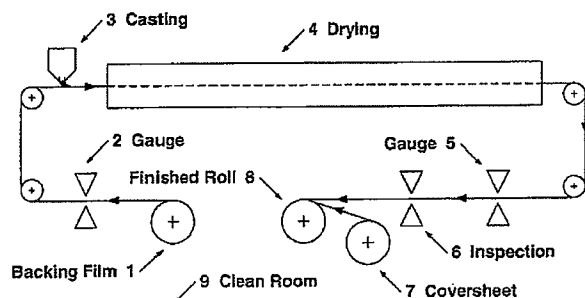
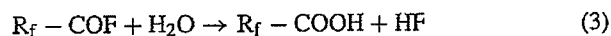
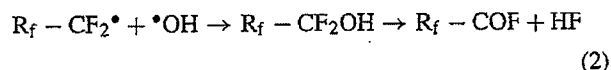
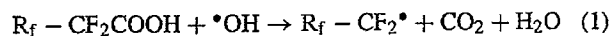


Fig. 2 Solution-casting process for Nafion® membranes

2. Experimental

2.1. Polymer chemical stability measurements

A sample of Nafion® membrane is treated in a solution of 30% hydrogen peroxide containing 20 ppm iron (Fe^{+2}) salts at 85 °C for 16–20 h. The resulting solution is checked for fluoride ion content using a fluoride specific ion electrode. The same membrane sample is treated two additional times, each treatment using fresh peroxide and iron. The results are recorded as the “total milligrams of fluoride per gram of sample” generated during the three treatment cycles. For membrane operating in fuel cells, the fluoride loss rate is reported as “micromoles fluoride ion per gram of sample per hour”.

2.2. Viscosity measurements

Dispersion viscosity is measured using a Brookfield (Middleboro, MA) digital viscometer model LVDVIII+ employing a wide gap concentric cylinder geometry. Using the SC4 series spindles and small sample adapter connected to a temperature controlled water bath (VWR), samples were equilibrated at 25.0 ± 0.1 °C before measurements were taken. For those samples that showed shear-thinning behavior, observed viscosities and shear rates were corrected at the spindle wall using established power law relationships for viscosity, shear rate, and geometry [13]. Dispersion viscosity is reported at 40 s^{-1} shear rate.

2.3. Size exclusion chromatography (SEC)

SEC molecular characterization was performed using a size exclusion chromatograph equipped with a Waters (Bedford MA) 2410 refractive index (RI) detector, Waters 515 HPLC pump, Waters column heater, and Rheodyne injector with 200 μl sample loop. A Precision Detectors (Franklin MA) PD2020 light scattering (LS) detector with static light scattering at 15° and 90° ($\lambda = 800 \text{ nm}$) and dynamic light scattering (DLS) at 90° was installed within the 2410 for constant temperature control (40 °C). Samples were eluted through two Polymer Laboratories (Amherst MA) SEC columns (Plgel 10 μm MIXED-B LS) maintained at 50 °C. The LS detector millivolt output relative to ΔR_θ and inter-detector volume were calibrated from an average of six injections (100 μl of $\sim 2 \text{ mg ml}^{-1}$) of a narrow polystyrene standard (Aldrich, product/lot # 330345, $\text{MW} = 44,000 \text{ g mol}^{-1}$) using dimethyl formamide (DMF) as the mobile phase (0.6 ml min^{-1}).

2.4. Dynamic mechanical analysis (DMA)

The DMA responses were measured using a TA Instruments Model 2980. The test measurements used thick specimens prepared by pressure laminating eight-layers of the 2 mil Nafion® membrane at 1000 psi, 80 °C between DuPont

Kapton® polyimide film. Film specimens approximately $15 \times 7 \times 0.4 \text{ mm}^3$ were cut from multi-layer membrane laminate for tensile DMA measurements. The test specimen was equilibrated at ambient temperature and humidity, then clamped in the tensile fixture, which is flushed with dry Nitrogen and cooled to -100 °C. The test chamber's relative humidity was not controlled during the DMA tests. Small-amplitude oscillatory stresses were applied at a frequency of 10 Hz, while measurements were made of the storage modulus E' and loss modulus E'' (plus the derived loss tangent, $\tan \delta = E''/E'$) as a function of temperature. Each DMA test included a number of sequential heating cycles, where the maximum temperature for each cycle progressively extended to a higher maximum temperature.

2.5. Surface tension

The air-liquid (surface) tension for Nafion® polymer dispersions was measured at 23 °C using the Wilhelmy platinum plate method. The platinum plate is pre-cleaned by flame treatment. The sample liquid is placed in a clean glass vessel, free of contaminants that may effect the surface tension of the liquid. The platinum plate (40 mm wide \times 0.2 mm thick \times 10 mm high) is attached to a force measuring device (Kruss K100 Tensiometer) and brought down into contact with the surface of the liquid being measured, along the 40 mm \times 0.2 mm bottom edge. The plate first is submerged below the surface of the liquid to a depth of 2.0 mm to wet the plate, and then pulled back to within 10 μm of the liquid's surface. The force of the liquid pulling down on the plate (the liquid's Wilhelmy force) is measured 60 s after the plate has stopped moving. The surface tension is the Wilhelmy force divided by the wetted length of the plate (its perimeter of 80.4 mm). The cited surface tensions are averages of three measurements, and reported in milliNewton per meter (mN m^{-1}).

2.6. Contact angle

The contact angle data for Nafion® PFSA Membranes was obtained with a Kruss Automated Goniometer DSA10, using an environmental chamber equipped with a dew point sensor to monitor and control conditions. Dew point was set at 12 °C for measurements at 23 °C, which yielded relative humidity of 50% at 23 °C. For each drop of water placed on a sample membrane, contact angles were measured every 5 s for 30 min. The reported “average” contact angle was based on the average of contact angle measurements for five drops of water placed on a particular sample, as a function of time after droplet placement.

2.7. Electrical shorts tolerance

A resistivity test measures the membrane's electrical shorts tolerance caused by penetration of surface fibers

from the gas diffusion layer. The test is performed in a constant humidity, constant temperature room with the samples conditioned at least 24 h before testing. The test apparatus consists of the inner elements of a single fuel cell, namely, the top and bottom electrode plates with lead wires and the top and bottom Pocco graphite flow fields. These elements sit on a rigid base in a constant rate of extension (CRE) test machine and are compressed with a 25.4 mm diameter ball mounted in the center of a 6.35 mm thick rigid steel plate. The ball is pushed by a rod attached to the load cell, so the plate remains parallel to the assembly. The DC resistance of the stack is measured across the electrode plates using an ohmmeter. A square, 50.8 mm \times 50.8 mm, of a gas diffusion backing (GDB) material is placed on the bottom flow field with the microporous layer facing up. The membrane is placed over the GDB and a second GDB piece is placed with the microporous layer facing down, over the membrane. The top flow field is then placed on top. The stack is centered over the bottom electrode plate and covered with the top electrode plate with the insulated side up. The CRE machine is closed so that the load cell just begins to measure load. The ohmmeter is attached to the electrode plates and the stack assembly is left to reach equilibrium as the “capacitor” charges. The test begins once the resistance reading is stable. The CRE machine is closed at a rate of 0.635 mm min⁻¹. The resistance is recorded as a function of the applied load and the pressure causing an electrical short is reported. A “failure” occurs when the electrical resistance drops below 1000 Ω .

2.8. Accelerated lifetime

The “time to failure” in hours is measured using a single fuel cell apparatus and proprietary testing protocols. This test is used to compare membranes and MEA designs against each other in a simulated fuel cell environment.

3. Results and discussion

3.1. Polymer chemical stability

Previously, DuPont had determined that fluoropolymer endgroup reactions could be minimized during extrusion processes by pre-treating the polymer with elemental fluorine [14,15] to remove reactive endgroups and impart greater thermal stability. When Nafion[®] polymer was treated in a similar manner, the number of measurable endgroups was reduced by 61%, thus providing a good candidate for chemical stability testing. Using the peroxide stability test, this treated polymer was compared with a sample of the same polymer before treatment. After >50 h of exposure, there was a 56% decrease in total fluoride ion generated per gram of treated polymer, versus the non-treated polymer, as shown in Fig. 3.

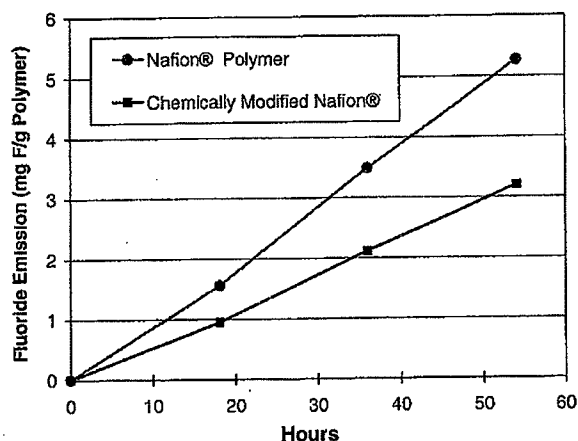


Fig. 3 Fluoride emissions for membranes made using standard and chemically modified Nafion[®] polymer

Recently, DuPont has developed proprietary protection strategies that substantially reduce both the number of polymer endgroup sites and their vulnerability to attack. Using ex situ accelerated degradation protocols, Fig. 4 shows that membranes made the modified polymer (type A and type B) exhibited 10 to 25 \times reduction in fluoride ion emissions when compared to the standard Nafion[®] N-112 membrane. The reduction in fluoride ion release was consistent with the reduction in the number of reactive polymer endgroups. It confirms that reactive endgroups are the vulnerable sites, and that the polymer can be effectively protected using DuPont's proprietary methods.

It should be noted that the ex situ accelerated degradation tests do not necessarily correlate to fuel cell accelerated degradation results. In one case, when membranes prepared from treated and non-treated polymer were tested in a fuel cell configuration using accelerated operating conditions, both membranes generated similar amounts of fluoride ion. Furthermore, clear relationships between accelerated test

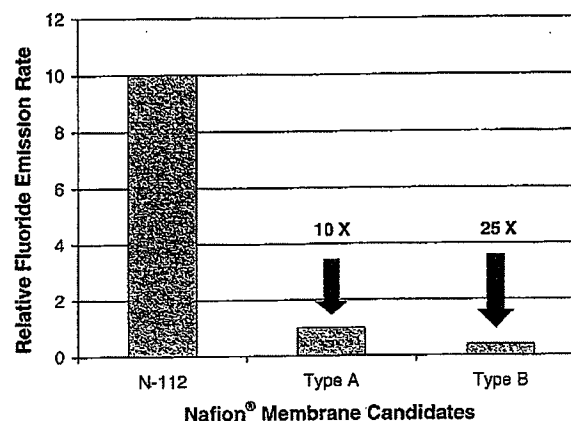


Fig. 4 Reduction in fluoride emissions for developmental Nafion[®] membranes made using DuPont's proprietary protection strategies

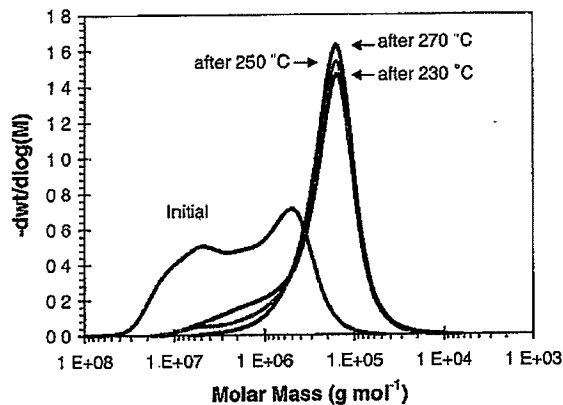


Fig. 5. Change in molar mass distributions after heating dispersions at progressively higher temperatures.

protocols and real-time fuel cell operating conditions have yet to be resolved satisfactorily.

DuPont continues to investigate those conditions present during PEM fuel cell operation which initiate F^- formation, including both initial and long-term release rates. The analysis includes identifying PFSA polymer and membrane features susceptible to attack, and subsequent modifications to minimize and/or eliminate polymer stress and degradation. In addition, the scope and range of fuel cell operating conditions are being assessed for their combined effect on fuel cell performance and membrane durability, including polymer structure and endgroups.

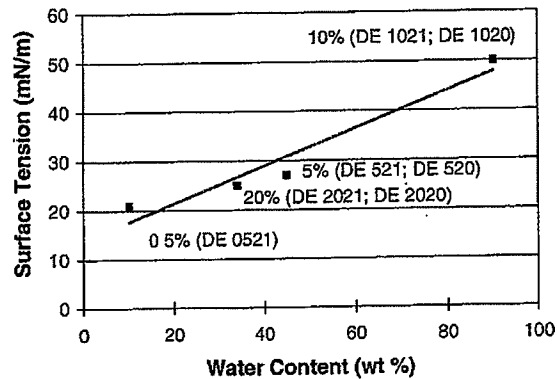


Fig. 6. Surface tension measurements Nafion® polymer dispersions.

3.2. Nafion® PFSA polymer dispersions

Size exclusion chromatography–low angle laser light scattering (SEC–LALLS) has been used to show that observed aqueous dispersion viscosities were related to an “apparent” molar mass, as a result of a process dependent aggregation phenomenon. Typical viscosities are between 4 and 5 cP for the nominal 10% solids aqueous dispersions at the time of manufacture.

As seen in Fig. 5, there was a noticeable high molar mass shoulder due to the aggregate structure in the mass distribution of the “as made” dispersion. On heating the aqueous dispersions to high temperatures, the aggregate structure was irreversibly broken down resulting in narrower

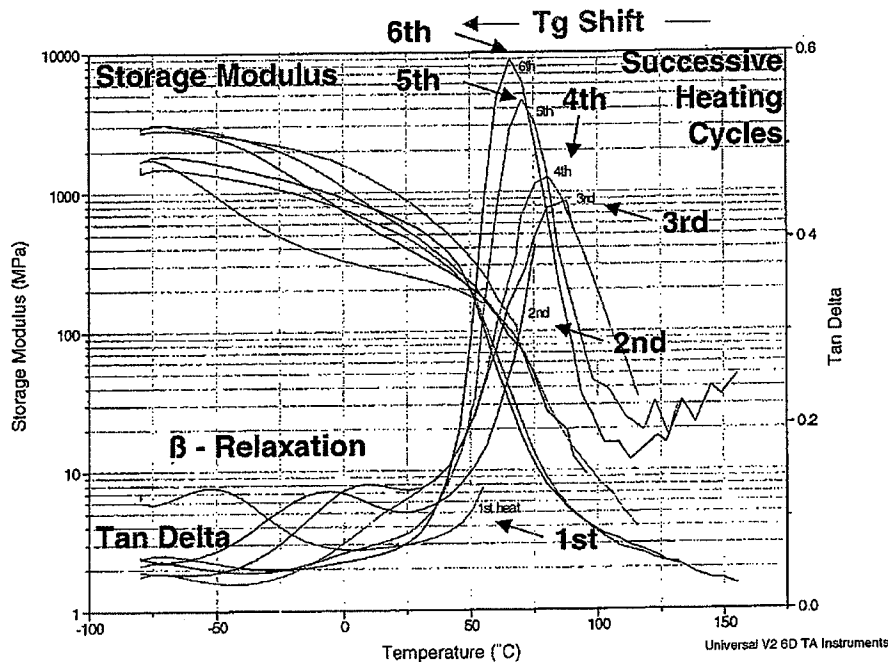


Fig. 7. DMA response data for NR-112 solution-cast membrane

mono-modal distributions, which were similar for all dispersions. The high temperature heating reduced viscosities to approximately 2 cP. Interestingly, limited two-angle dependant light scattering measurements had indicated a linear relationship between the radius of gyration and molar mass for the aggregate portion of the “as made” distribution. This was consistent with previous research, which concluded that the dispersion particle shape was anisotropic, possibly rod and/or ribbon form.

This evidence suggested a model for Nafion® dispersions where elongated, charge stabilized particles exist on a three-dimensional lattice with the particle centers of mass at the lattice points. Furthermore, for dispersions that had even greater aggregate distributions, viscosity-shear thinning might result as a consequence of particle overlap and lattice deformation in a shear field.

Based on this work and other process developments, DuPont has introduced a new generation of polymer dispersions offering increased acid capacities, reduced metal ion content, and improved color and viscosity stability. The new dispersions are available in 5, 10 and 20% polymer content, two acid capacity levels, and mixed 1-propanol/water and water-only dispersions.

The surface tension of a polymer dispersion is an important consideration for optimization of catalyst coatings and efficiencies, coating adhesion, and membrane formation from dispersion. The surface tensions for the Nafion® polymer dispersions are reported in Fig. 6. The “percent (%)” value next to each data point indicates the dispersion’s polymer content, which when added to the wt % water (indicated on the graph) and wt % alcohol (inferred) equal 100%. As expected, the aqueous dispersions exhibit the highest surface tensions (50 mN m^{-1}); while increasing alcohol content depresses the surface tension. For example, DE 2021 (containing 20% polymer, 34% water and 46% 1-propanol) has a surface tension of 25 mN m^{-1} . The range of possible surface tensions offers broad formulation capabilities for MEA fabrication.

3.3 Nafion® PFSA solution-cast membranes

The tensile storage modulus exhibits three distinct relaxation modes (α , β , γ) as a function of temperature, and all are sensitive to water content. Kyu and Eisenberg [16] attribute the α -relaxation to the glass relaxation of the hydrophilic phase domains, and the β -relaxation to the glass relaxation for the fluorocarbon phase domains. In Fig. 7, the DMA response for solution-cast membrane shows the dominant α -relaxation (T_g) shifting to lower values with successive heating cycles (and decreasing water content). The T_g starts at 85°C and decreases to approximately 65°C during the six successive cycles. This response is similar to that of extrusion-cast membrane. The β -relaxation (-50 to 10°C) is stronger for solution-cast membrane (starting from humidified samples), but the difference attenuates after heating above 100°C in dry N_2 . The γ -relaxation, which occurs

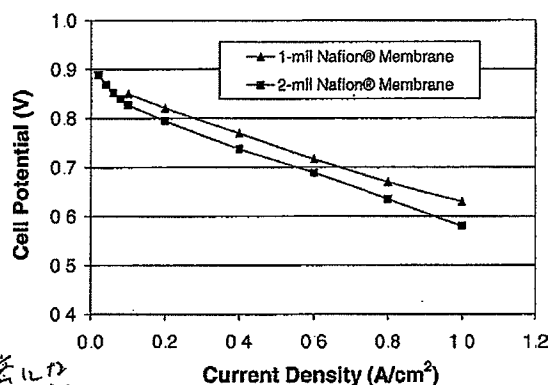


Fig. 8 Single cell MEA performance at 65°C , 100% RH, 0 psig, H_2/Air (80/60%), 0.7 mgPt cm^{-2} total loading.

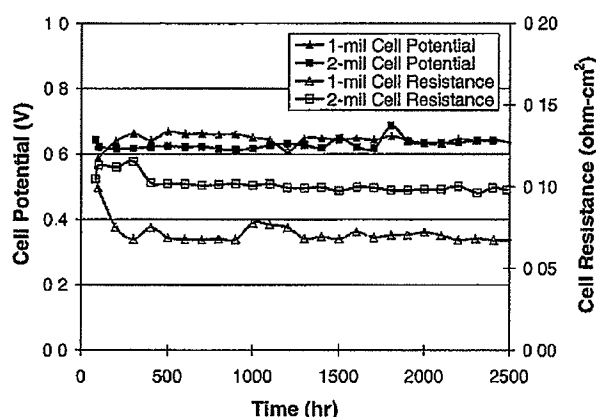


Fig. 9 MEA life test data: cell potential and resistance at 0.8 A cm^{-2} unchanged for 2500 h.

below -80°C , was not measured. When the membrane sample is re-equilibrated to the initial ambient humidity, the DMA responses return to their original starting values.

Figs. 8 and 9 document single cell performance and life test data for DuPont Fuel Cells three-layer MEAs fabricated

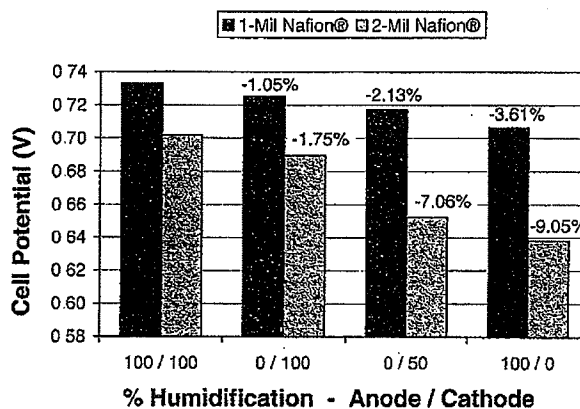


Fig. 10. Humidification effect on MEA performance at 80°C , 25 psig, H_2/Air (50/50%), 0.8 A cm^{-2} , 0.7 mgPt cm^{-2} total loading.

with catalyst-coated 1 and 2 mil Nafion® membranes, and using commercially available gas diffusion media.

The fuel cell performance gain for 1 mil membrane over 2 mil membrane at high current density operation under reduced humidification is more than the contribution from the cell resistance differential alone. This gain represents enhanced water back-diffusion for the thinner membrane [17]. The 1 mil membrane experiences a lower voltage decline over the range of reduced anode and cathode humidification levels, as shown in Fig. 10. This provides a 10% increase in fuel cell power output for MEAs using the 1 mil membrane versus the 2 mil membrane.

Fabrication requirements, such as lamination, reinforcement, surface coatings, and other membrane related processes rely heavily on interfacial strength, which can be optimized by matching cohesive energies of adjacent layers. This attribute for Nafion® membranes can be estimated by measuring water contact angles. For this evaluation, membrane samples were tested “as made”, “annealed” at 130 °C for 30 min in a dry nitrogen purged environment, and “boiled” in D.I. water for 30 min and blotted dry prior to testing.

Fig. 11 illustrates the degree of change in surface characteristics achievable by various membrane treatments; as well as how the surface characteristics change with time for the various treatments. The water contact angle responses for the extruded (N-112) and solution-cast (NR-112) membrane samples were identical for the “annealed” state, but very different for the “as made” and “boiled” states. This behavior may be influenced by the membrane’s prior

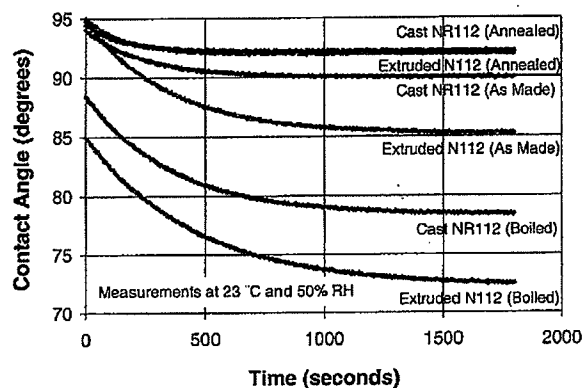


Fig. 11 Water contact angle for “as made” and treated 2.0 mil Nafion® membranes

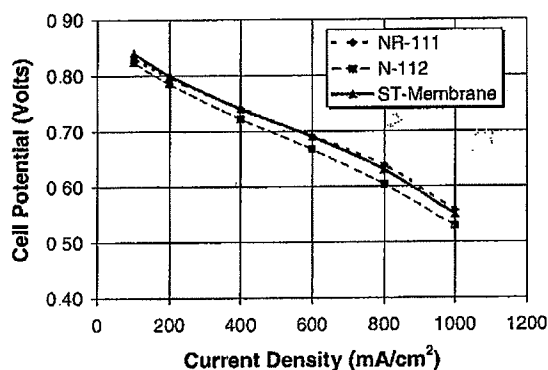


Fig. 12. Single cell MEA performance at 65 °C, 100% RH, 0 psig H₂/Air (80/60%), 0.7 mgPt cm⁻² total loading

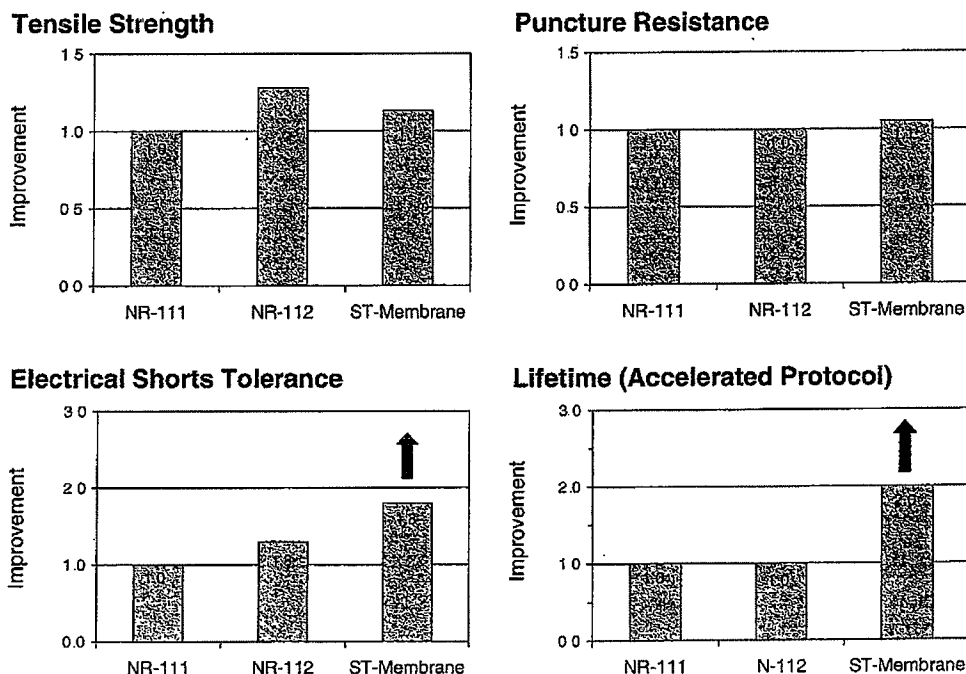


Fig. 13 Improvement comparisons between solution-cast and strengthened membranes

thermal history (melt extrusion versus solution-cast) and water content, which is higher for the solution-cast (NR) membrane in the “as made” and “boiled” states; but very similar for both membranes in the “annealed” state.

3.4. Nafion® ST membranes

DuPont has developmental programs focused on improving membrane mechanical durability as measured by several physical property and performance indicators. These include mechanical durability, as measured by tensile strength, reduced dimensional change, puncture resistance, electrical short tolerance, and lifetime (voltage over time using accelerated test protocols).

MEAs made with Nafion® ST membrane by DuPont Fuel Cells have demonstrated improved mechanical durability and lifetime, with fuel cell performance similar to Nafion® NR-111 as shown in Fig. 12.

Tensile strength and puncture resistance performance were similar for both solution-cast and ST Membrane. However, compared to NR-111, the ST membrane has 50–80% improvement in electrical shorts tolerance and 2× extended lifetime as measured using DuPont’s accelerated test protocol. Fig. 13 summarizes these comparisons.

The reported polymer and membrane improvements are undergoing validation and qualification in several commercial applications. Using the “voice of the customer”, DuPont is determining what additional membrane improvements are needed for MEA fabrication and fuel cell applications based on customer evaluations and durability feedback. The improvements will incorporate chemical stability features as they are developed for both the Nafion® polymer and membrane.

4. Conclusions

DuPont Fuel Cell’s polymer, dispersion, solution-cast and extrusion-cast membrane technologies provide the fuel cell industry with more efficient and flexible production capabilities, specialized membrane features, and reduced overall MEA fabrication costs. Today, DuPont is operating large-scale, thin membrane production facilities to provide the long-term projected membrane volumes at automotive quality standards and customer performance targets.

Ongoing polymer and membrane improvement programs are focused on providing the required performance, mechanical durability, and chemical stability necessary for successful PEM fuel cell applications. Fundamental research has enabled processing advancements for Nafion® polymer dispersions as well as formulation choices for improved fuel cell membrane fabrication and performance. Developmental ST membrane has shown favorable response based on our current mechanical durability indicators. The pipeline of new products and features is evidence of DuPont Fuel

Cell’s commitment and leadership in supplying membranes and components to the fuel cell industry.

Acknowledgements

DuPont CR&D: David Londono and Steve Mazur; and DuPont Fuel Cells: Jayson Bauman, Gonzalo Escobedo, Kim Raiford, Eric Teather, Elizabeth Thompson and Mark Watkins. Nafion® is a DuPont registered trademark for its brand of perfluorinated polymer products made and sold only by E.I. du Pont de Nemours and Company.

References

- [1] D.J. Connolly, W.F. Gresham, Fluorocarbon Vinyl Ether Polymers, US Patent 3,282,875 (1 November 1966).
- [2] R.A. Smith, Coextruded Multilayer Cation Exchange Membranes, US Patent 4,437,952 (20 March 1984).
- [3] C. Preischl, P. Hedrich, A. Hahn, Continuous Method for Manufacturing a Laminated Electrolyte and Electrode Assembly, US Patent 6,291,091 B1 (18 September 2001).
- [4] J. Kohler, K.-A. Starz, S. Wittphal, M. Diehl, Process for Producing a Membrane Electrode Assembly for Fuel Cells, US Patent 2002/0064593 A1 (30 May 2002).
- [5] W.G. Grot, Process for Making Liquid Composition of Perfluorinated Ion Exchange Polymer, and Product Thereof, US Patent 4,433,082 (21 February 1984).
- [6] D.E. Curtin, E.G. Howard Jr., 1997, Compositions Containing Particles of Highly Fluorinated Ion Exchange Polymer, US Patent 6,150,426 (21 November 2000).
- [7] W.G. Grot, G. Rajendran, Membranes Containing Inorganic Fillers and Membrane and Electrode Assemblies and Electrochemical Cells Employing Same, US Patent 5,919,583 (6 July 1999).
- [8] W.G. Grot, Process for Making Articles Coated with a Liquid Composition of Perfluorinated Ion Exchange Resin, US Patent 4,453,991 (12 June 1984).
- [9] S. Banerjee, Fuel Cell Incorporating a Reinforced Membrane, US Patent 5,795,668 (18 August 1998).
- [10] J.E. Spethmann, J.T. Keating, 1998, Composite Membrane with Highly Crystalline Porous Support, US Patent 6,110,333 (29 August 2000).
- [11] R. Baldwin, M. Pham, A. Leonida, J. McElroy, T. Nalette, Hydrogen-oxygen proton-exchange membrane fuel cells and electrolyzers, *J. Power Sources* 29 (1990) 399–412.
- [12] M. Pianca, E. Barchiesi, G. Esposito, S. Radice, End groups in fluoropolymers, *J. Fluorine Chem.* 95 (1999) 71–84.
- [13] H.A. Barnes, J.F. Hutton, K. Walters, *An Introduction to Rheology*, Elsevier, New York, 1989.
- [14] R.A. Morgan, W.H. Sloan, Extrusion Finishing of Perfluorinated Copolymers, US Patent 4,626,587 (2 December 1986) JP 56-171110 A
- [15] J.F. Imbalzano, D.L. Kerbow, Stable Tetrafluoroethylene Copolymers, US Patent 4,743,658 (10 May 1988) JP 56-174822 A
- [16] T. Kyu, A. Eisenberg, in: A. Eisenberg, H.I. Yeager (Eds.), *Mechanical Relaxations in Perfluorosulfonate Ionomer Membranes*, Perfluorinated Ionomer Membranes ACS Symposium Series 180, American Chemical Society, Washington, DC, 1982, (Chapter 6).
- [17] J.J.P. Freire, E.R. Gonzalez, Effect of membrane characteristics and humidification conditions on the impedance response of polymer electrolyte fuel cells, *J. Electroanal. Chem.* 503 (2001) 57–68.

End groups in fluoropolymers

Maurizio Pianca^{*}, Emma Barchiesi, Giuseppe Esposto, Stefano Radice

Ausimont S.p.A., Via S Pietro 50/a, 20021 Bollate Milano, Italy

Abstract

IR and NMR spectroscopies are the most important techniques used to identify and quantify end groups in fluoropolymers. We review here some literature studies about the characterisation of end groups in some fluoropolymers based on tetrafluoroethylene, vinylidene fluoride and vinyl fluoride, adding the contribution of our investigation on the matter. © 1999 Elsevier Science S.A. All rights reserved.

Keywords: Fluoropolymers; End groups; IR spectroscopy; NMR spectroscopy

1. Introduction

It is normally accepted that end groups have no significant influence on macroscopic properties of polymers, because their weight is negligible as compared with the whole mass of the polymer and because energy values for bonds in end groups and in the constitutive units are practically equal.

This statement cannot be applied to perfluoro polymers where hydrogen containing end groups (produced for instance by a hydrogen containing peroxide initiator) do have a definite influence on their thermal stability, as can be expected by comparing the bond strength of C–H with C–F (about 410 and 460 kJ/mol, respectively).

It has been demonstrated that also hydrogen and fluorine containing polymers, for example poly(vinylidene) fluoride (PVDF), are influenced, as far as thermal stability and fire resistance are concerned, by the end groups generated in the presence of different initiators. Since in this case the relative strength of C–H and C–F bonds cannot be the determining factor, this unexpected behaviour was attributed to different degradation mechanisms induced by the nature of the end groups [1].

In PVDF other properties, such as fluidity and electrical conductivity, were demonstrated to be significantly influenced by end groups.

End groups can also determine the crystallisation kinetics from the melt of thermoplastic fluoropolymers, and hence the processing and end-use properties [2].

Being aware of the importance of end groups in determining the properties of fluoro polymers, we will review here the studies about their identification and quantitative determi-

nation in some commercial fluoropolymers adding, where possible, the original results of our work on this subject. All literature data reported herewith have been experimentally confirmed in our laboratories.

We will consider the following polymers:

- poly(tetrafluoroethylene) (PTFE) and TFE based thermoplastic fluoropolymers,
- poly(vinylidene fluoride) (PVDF) and VDF based fluoroelastomers, and
- poly(vinyl fluoride) (PVF).

2. PTFE and TFE based thermoplastic fluoropolymers

The end groups identified in thermoplastic fluoropolymers can be generated during the polymerisation process (initiator, transfer agent, solvent, contaminants, etc.), or by handling of the polymer (ageing, heating, extrusion, chemical reactions and so on).

IR spectroscopy is a particularly useful technique in the determination of end groups in TFE based polymers, since they are insoluble in common solvents. Moreover, many functional groups show absorptions in spectral regions that are free from the main absorption bands of the polymer. One of the major features of infrared Fourier transform spectroscopy is the high sensitivity due to the high energy available and the possibility to enhance the signal to noise ratio by increasing the number of scans. In fact it is possible to evaluate end groups concentration in the range 10^{-3} – 10^{-5} mol/kg.

In our laboratories IR spectra of polymers have been recorded with a Nicolet 20 SX or a Nicolet 850 FT-IR instrument. Collection parameters included 2 cm^{-1} resolution and 500 scans. Spectra have been elaborated on a PC

^{*}Corresponding author.

with Lab Calc software (Galactic Industries). The samples have been analysed as pellets obtained by cold pressing, while model compounds have been analysed in the best condition according to their physical nature. Since most of the results have been obtained through spectral subtraction, as a reference sample we used a polymer exposed for several hours to elemental fluorine at 100–150°C; such a treatment transforms almost all end groups to perfluoromethyl groups [3,8].

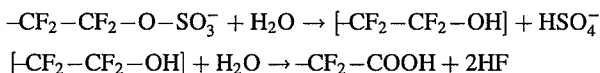
To assign the absorption bands to distinctive functional groups, we used both literature data [3,4,7–16] and model compounds. Sometimes, we performed simple chemical reactions to confirm assignments. Model compounds have been used for the determination of extinction coefficients. The data here reported have been obtained for PFA polymers (tetrafluoroethylene/perfluoropropylvinylether copolymers TFE/PFPVE). These results can be extended to other TFE based copolymers.

The following end groups have been identified:

- carboxylic acid ($-\text{CF}_2-\text{COOH}$),
- amide ($-\text{CF}_2-\text{CONH}_2$),
- perfluorovinyl ($-\text{CF}_2-\text{CF}=\text{CF}_2$),
- acyl fluoride ($-\text{CF}_2-\text{COF}$),
- difluoromethyl ($-\text{CF}_2-\text{CF}_2\text{H}$), and
- ethyl ($-\text{CF}_2-\text{CH}_2-\text{CH}_3$).

2.1. Carboxylic acid groups

These groups are generated in the polymer when a persulphate initiator is used, according to the following [4]:

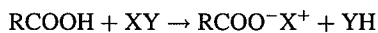


Carboxylic groups are identified by IR spectroscopy by the following group frequencies due to the O–H and the C=O stretching:

- 3557 cm^{-1} (sharp, O–H stretching, free),
- $3300\text{--}3000\text{ cm}^{-1}$ (broad, O–H stretching, bonded),
- 1813 cm^{-1} (sharp, C=O stretching, free), and
- 1775 cm^{-1} (C=O stretching, bonded).

The nature of the observed bands was verified by means of chemical reactions and model compounds.

The most simple reaction of a carboxylic group is its salification by a base.



This reaction from the spectroscopic point of view leads to the disappearance of both O–H and C=O stretching bands and to the appearance of new bands due to the in phase and out of phase $-\text{COO}^-$ stretching vibration.

A polymer powder containing $-\text{COOH}$ groups, exposed to the vapours evolved by an ammonia solution, showed the decreasing of the 1813 and 1775 cm^{-1} bands. The appear-

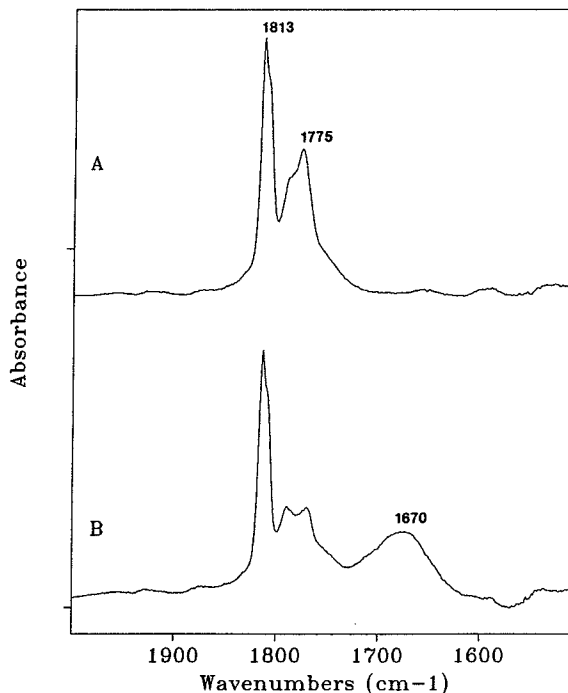


Fig. 1. (A) IR absorption bands (C=O stretching region) due to carboxylic end groups in a PFA polymer. (B) The same spectral regions observed after exposure to ammonia.

ance of a broad absorption at about 1675 cm^{-1} is due to the out of phase stretching of the $-\text{COO}^-$ group (Fig. 1).

Changes in the $3300\text{--}3000\text{ cm}^{-1}$ region are mainly attributed to the complex pattern due to $(\text{NH}_4)^+$ stretching.

The salification reaction is reversible. As a matter of fact, by exposing the powder to HCl vapours we observe the increasing of the bands at 3557 , 1813 and 1775 cm^{-1} and the decreasing of the 1673 cm^{-1} absorption.

Carboxylic groups can decompose by thermal treatment following different mechanisms:

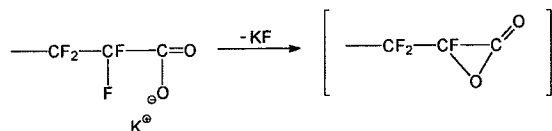
- $-\text{CF}_2-\text{CF}_2-\text{COOH} \rightarrow -\text{CF}=\text{CF}_2 + \text{CO}_2 + \text{HF}$
- $-\text{CF}_2-\text{CF}_2-\text{COOH} \rightarrow -\text{CF}_2-\text{COF} + \text{HF} + \text{CO}$
- $-\text{CF}_2-\text{CF}_2-\text{COOH} \rightarrow -\text{CF}_2-\text{CF}_2\text{H} + \text{CO}_2$

Mechanism (a) is observed for instance during press treatment at 380°C for some minutes. We noted the decreasing of the absorptions due to carboxylic groups and the formation of a band at 1784 cm^{-1} due to perfluorovinyl groups [3].

Mechanism (b) is quite interesting and deserves a more detailed discussion. It has been observed during industrial extrusions of perfluoropolymers manufactured by aqueous emulsion polymerisation with $\text{K}_2\text{S}_2\text{O}_8$ as initiator. In the IR spectra of the extruded items we observed a substantial decrease of the absorptions due to the carboxylic groups and the formation of a band at 1884 cm^{-1} attributable to the $-\text{CF}_2-\text{COF}$ end groups. The same mechanism was observed

by heating at 350°C a sample of γ irradiated PTFE, that showed a high content of $-\text{COOH}$ end groups; in the gas evolved by the sample were identified HF and CO. A similar carboxylate thermolysis with CO elimination has been described in [5].

Since the carboxylic groups could be present either as K^+ salts or in the protonated form, a unimolecular reaction pathway was proposed similar to that shown in the following scheme.



KF and/or HF, eliminated α to the carbonyl, results in a zwitterionic intermediate which can evolve into a cyclic form. Upon heating, loss of carbon monoxide from the cyclic intermediate results in the observed end groups. This mechanism is not unusual and closely resembles the thermal extrusion of difluorocarbene from hexafluoropropene oxide to give acetyl fluoride. Very recently a similar mechanism has been claimed to account for the vacuum thermolysis of sodium fluoropropionate derivatives to give a trifluoroacetate ester [6].

Mechanism (c) is followed when the carboxylate end group is in ionic form and the polymer is treated with water at 210–250°C [7,9–12].

As a model compound for the determination of molar extinction coefficients of the carboxylic group bands, we used perfluorooctanoic acid. IR spectra of this compound have been recorded as solutions at different concentration in a perfluorinated fluid (Galden® D100). As expected, the bands of bonded carboxylic groups decrease with dilution up to complete disappearance. Molar extinction coefficients relative to the 3557, 1813 and 1775 cm^{-1} bands have been determined and reported in Table 1.

In Table 1 we have also collected all the molar extinction coefficients determined experimentally as reported further in this paper. Literature data, as for example in [8,9] are consistent with our results.

2.2. Amide groups

Amide end groups can be generated during the polymerisation step when ammonium salts are used. Their presence is revealed by four bands at 3555, 3438, 1768 and 1587 cm^{-1} . We assign the two high frequencies to asymmetric and symmetric NH_2 stretching of R_fCONH_2 groups, the 1768 cm^{-1} band to C=O stretching and the 1587 cm^{-1} to the N–H deformation.

The assignment was confirmed by means of hydrolysis and pyrolysis reactions:

- acid hydrolysis: $-\text{CF}_2\text{CONH}_2 + \text{H}_2\text{O} + \text{HCl} \rightarrow -\text{CF}_2\text{COOH} + \text{NH}_4\text{Cl}$
- pyrolysis: $-\text{CF}_2\text{CONH}_2 \xrightarrow{\Delta} -\text{CF}_2-\text{C}\equiv\text{N} + \text{H}_2\text{O}$

Table 1

IR spectroscopy end groups assignments and extinction coefficients

Frequency (cm^{-1})	Group	Assignment	Extinction coefficient (l/mol cm)
3557	COOH	OH str.	165
3555	CONH ₂	NH ₂ asym. str.	220
3438	CONH ₂	NH ₂ sym. str.	220
3300–3000	COOH (H)	OH str.	Not available
3005	CF ₂ H	CH str.	351 ^a
3003	CH ₂ CH ₃	CH str.	34
1884	COF	CO str.	215
1813	COOH	CO str.	230
1784	CF=CF ₂	CC str.	455
1775	COOH (H)	CO str.	1700
1768	CONH ₂	CO str.	940
1670 (broad)	COO [−] X ⁺	COO [−] asym. str.	Not available
1587	CONH ₂	NH ₂ def.	220

Asymm. str.=asymmetric stretching.

Symm.str.=symmetric stretching.

Def.=deformation motion.

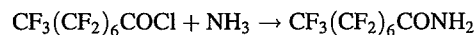
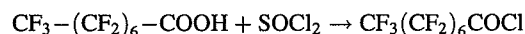
H=hydrogen bonded.

^a l/mol cm^2 , integrated absorbance data were used (see text).

Hydrolysis was carried out in a 20% hydrochloric acid boiling solution for 24 h. After the treatment the absorptions of the amide bands were decreased and the bands of the carboxylic group appeared (Figs. 2 and 3); NH_4Cl was also observed in the acid solution.

Pyrolysis experiments basically consisted in a thermal treatment at 360°C (2 h) in nitrogen atmosphere. IR spectra after this treatment show the decreasing of the amide absorptions and the appearance of a band at 2263 cm^{-1} due to $\text{C}\equiv\text{N}$ stretching.

As a model compound for the determination of the absorption coefficients we used perfluorooctanoic amide, prepared according to the following reactions:



The spectra of this compound have been recorded as solution in Galden® D100.

2.3. Perfluorovinyl groups

In the IR spectra of some PFA polymers we have observed a band at 1784 cm^{-1} (Fig. 4). The same absorption was observed during the thermal degradation of $-\text{COOH}$ end groups. This band is not affected by the ammonia vapours treatment; accordingly we attributed it to perfluorovinyl double bond stretching.

The attribution has been confirmed by examining the IR spectrum of perfluoro-1-heptene; this model compound was also used, as a Galden® D100 solution, to determine the extinction coefficient of the 1784 cm^{-1} band (Table 1).

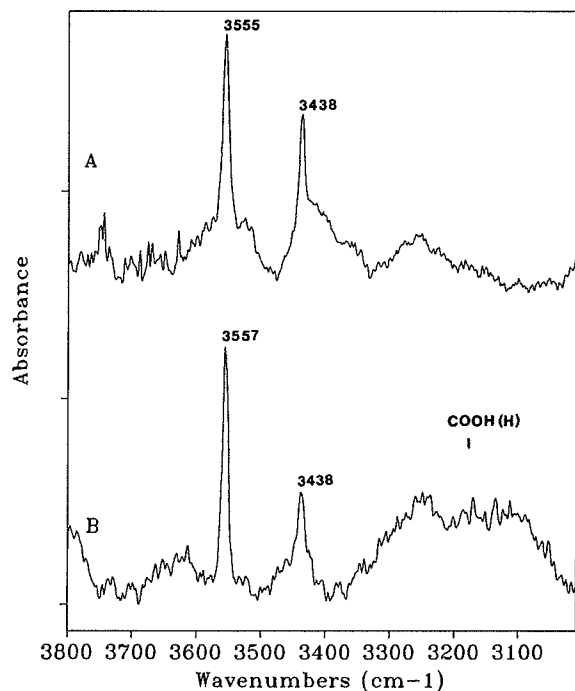


Fig. 2. (A) IR absorption bands (N–H stretching region) due to amidic end groups in a PFA polymer. (B) The same spectral regions observed after acid hydrolysis.

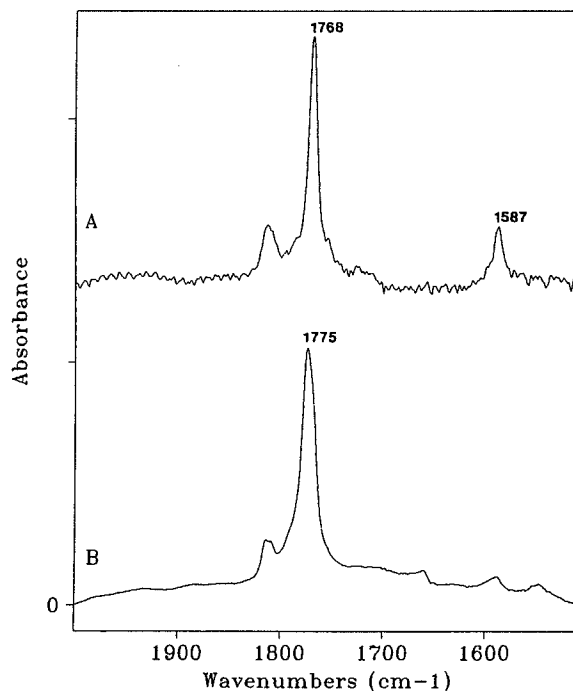
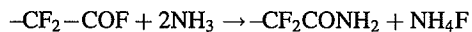


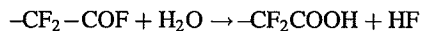
Fig. 3. (A) IR absorption bands (C=O stretching region) due to amidic end groups in a PFA polymer. (B) The same spectral regions observed after acid hydrolysis.

2.4. Acyl fluoride groups

In the IR spectra of some extruded TFE perfluorinated copolymers we noticed a band at 1884 cm^{-1} (Fig. 5(A)), which is assigned to C=O stretching in $R_f\text{COF}$ groups. By exposition to ammonia vapours we transformed the $R_f\text{COF}$ groups into amide groups (Fig. 5(B)) according to the following reaction:

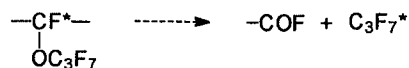


Exposition to water vapour leads to carboxylic groups:



We proceeded in the evaluation of the $-\text{COF}$ extinction coefficient indirectly, determining the content of the $-\text{COOH}$ groups after complete hydrolysis of the perfluoro-acyl groups.

It is worth enough to say that in PFA copolymers $-\text{CF}_2\text{COF}$ end groups can also be generated during polymerisation through the following radical rearrangement:



2.5. Difluoromethyl groups ($-\text{CF}_2-\text{CF}_2\text{H}$)

When these end groups are present, they give rise to weak absorptions in the CH stretching region [7,9–12]. Actually,

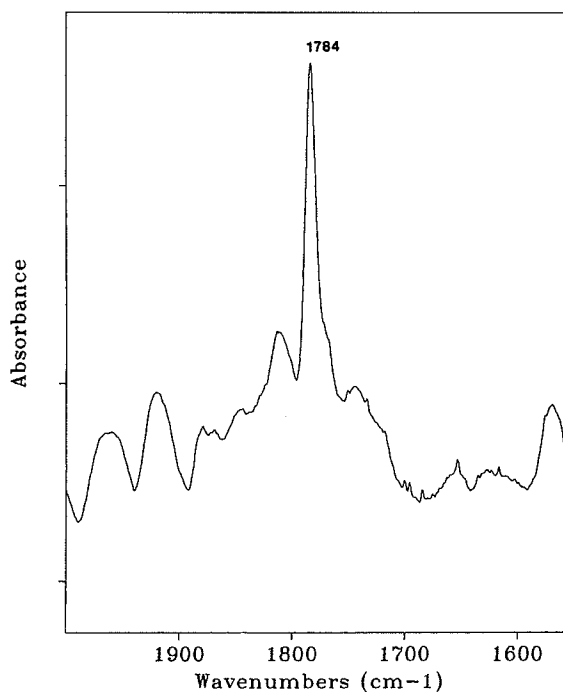


Fig. 4. IR spectrum (C=C stretching region) of a PFA polymer (perfluorovinyl end groups).

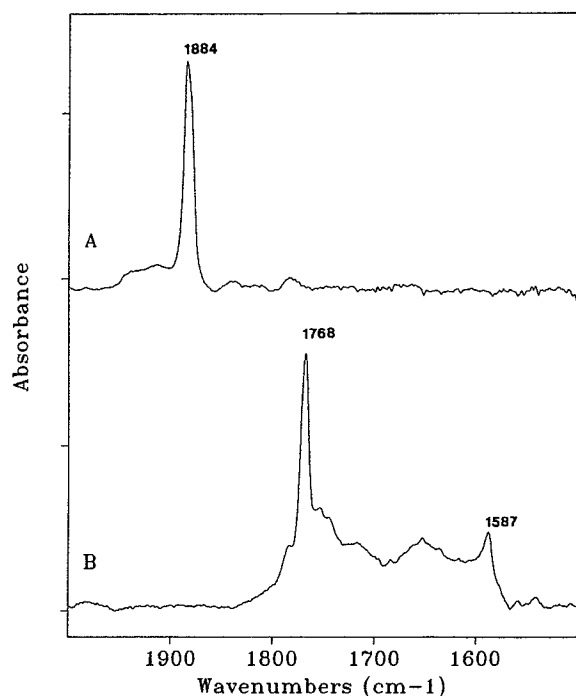


Fig. 5. (A) IR spectrum (C=O stretching region) of a PFA polymer (acylfluoride end groups). (B) The same spectral regions observed after exposure to ammonia and water vapours.

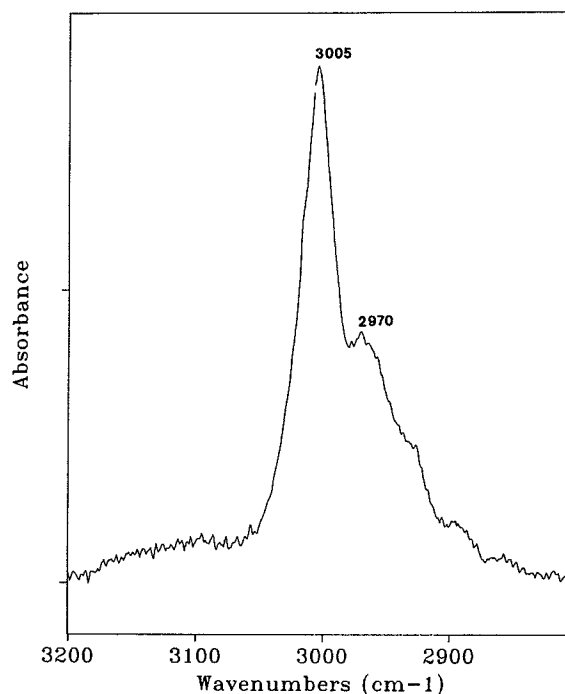


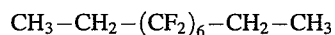
Fig. 6. IR spectrum (C-H stretching region) of a PFA sample (difluoromethyl end groups).

we observe two bands at 3005 and about 2970 cm^{-1} (Fig. 6). We used as a model compound $\text{CF}_2\text{Cl}-(\text{CF}_2)_6-\text{CF}_2\text{H}$. Its IR spectrum shows these two bands in the CH stretching region. The presence of two bands is justified by the existence of two different conformers. The hypothesis has been confirmed recording IR spectra at different temperatures (from room temperature to about 150°C). A Van't Hoff plot (Fig. 7) gave an energy difference for the two conformers of about 0.5 Kcal/mol.

In this case the integrated absorbance of the two bands (3005 and 2970 cm^{-1}) has been used to determine the extinction coefficient of $-\text{CF}_2\text{H}$ group. The result has been obtained using $\text{CF}_2\text{Cl}-(\text{CF}_2)_6-\text{CF}_2\text{H}$ in Galden® D100 solution and is reported in Table 1.

2.6. Ethyl groups ($-\text{CF}_2-\text{CH}_2-\text{CH}_3$)

By using ethane as a chain-transfer agent in the emulsion polymerisation of TFE based thermoplastic fluoropolymers, we expect to obtain $-\text{CF}_2-\text{CH}_2-\text{CH}_3$ end groups. As a matter of fact in the complex pattern observed in the CH stretching region of the IR spectra of these polymers we identify three bands at 3003, 2960 and 2900 cm^{-1} (Fig. 8). The assignment of the three bands to the ethyl groups is confirmed by the following model compound:



that has also been used to determine the extinction coefficient relative to the 3003 cm^{-1} band (Table 1).

3. Poly(vinylidene fluoride) (PVDF)

In many papers dealing with the investigation of PVDF microstructure by means of ^{19}F NMR spectroscopy, the presence of peaks which cannot be related to any units in the linear polymer chain is reported and generally attributed to impurities, oligomers, end groups or branching sites. Namely, some of these peaks have been assigned in [17]: the weak resonances at -100.3, -104.52 and 107.54 ppm have been associated to branched structures such as $-\text{CH}_2-\text{CF}_2-\text{CH}<$ or $-\text{CH}_2-\text{CF}_2-\text{CF}<$. However, the assignments are based only on the empirical rules for the calculation of chemical shifts developed by Murasheva et al. [18] and no proof of these assignments is given. Furthermore, in [19] the multiplet at -114.15 ppm, which is detectable in almost all PVDF ^{19}F NMR spectra, is attributed to an unidentified end group and in [20] the same signal is assigned to an impurity.

A paper [21] dealing with PVDF telomers (with number average molecular weights in the range 2000–3000) obtained using 1,2-dibromotetrafluoroethane as telogen in the presence of different initiators, gave the detailed ^{19}F and ^1H NMR information about end groups, originated by the

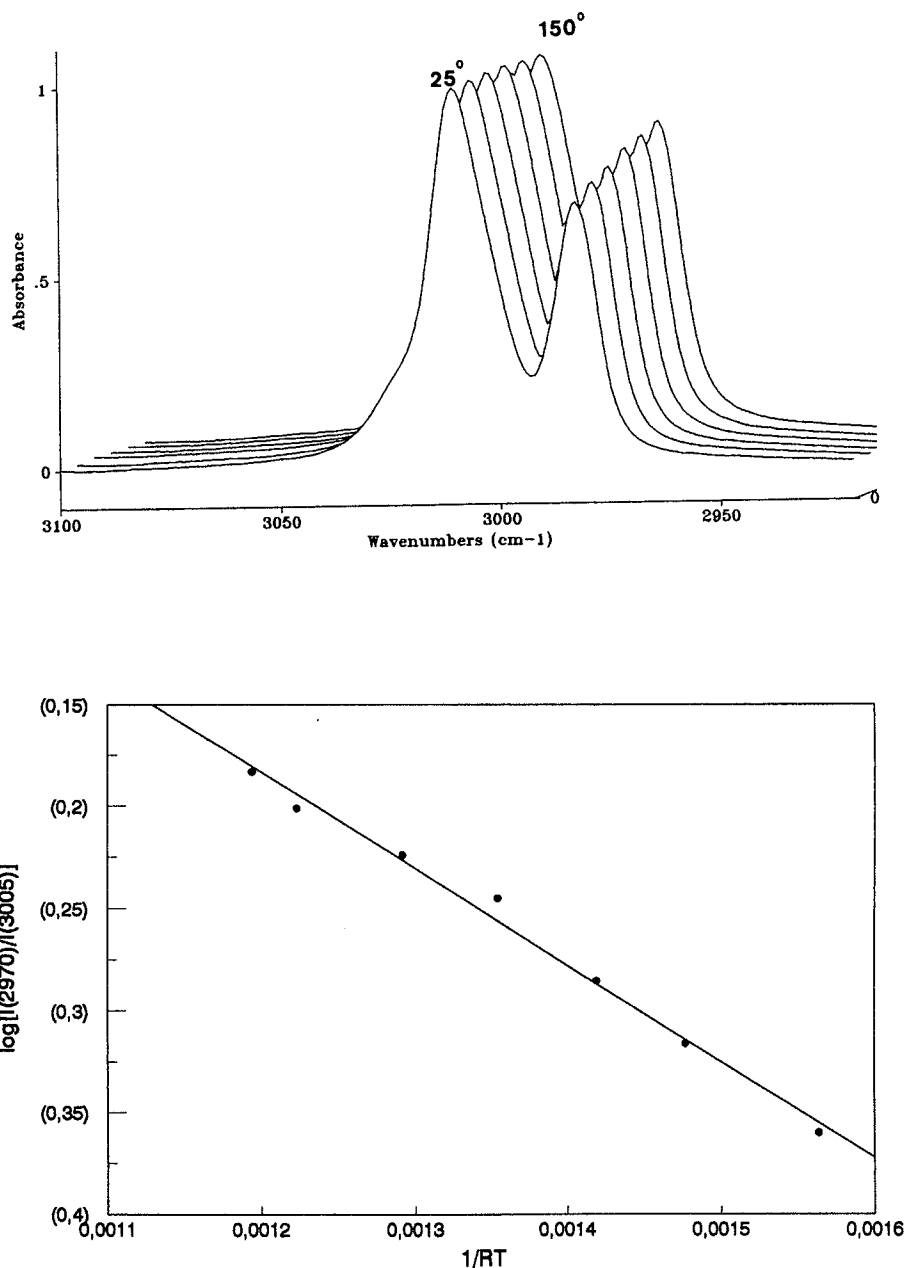


Fig. 7. Evolution of the IR spectrum (C–H stretching region) of $\text{CF}_2\text{Cl}-(\text{CF}_2)_6\text{CF}_2\text{H}$ as a function of temperature (20–150°C) and relative Vant'Hoff plot. $I(2970)$ and $I(3005)$ are the optical densities of the two bands.

initiator or by transfer reactions, reported at the beginning of Tables 2 and 3.

Assignments were performed by comparison of ^1H and ^{19}F NMR spectra and by the use of two-dimensional fluorine–fluorine chemical shift correlation spectroscopy (COSY).

Particular attention was paid to the signals attributed to $-\text{CF}_2-\text{CF}_2-\text{CH}_3$ and $-\text{CH}_2-\text{CF}_2\text{H}$ end groups, that are

present in the spectra of many authors, but had never been identified and often misinterpreted. These groups, whose concentration is strongly dependent on the type and concentration of initiator, may be due to hydrogen abstraction from either or both initiator molecules or PVDF chain.

In this latter case a possible mechanism to justify the presence of the $-\text{CF}_2\text{H}$ and the $-\text{CH}_3$ groups could be a short chain-branching process involving an intramolecular 1–5

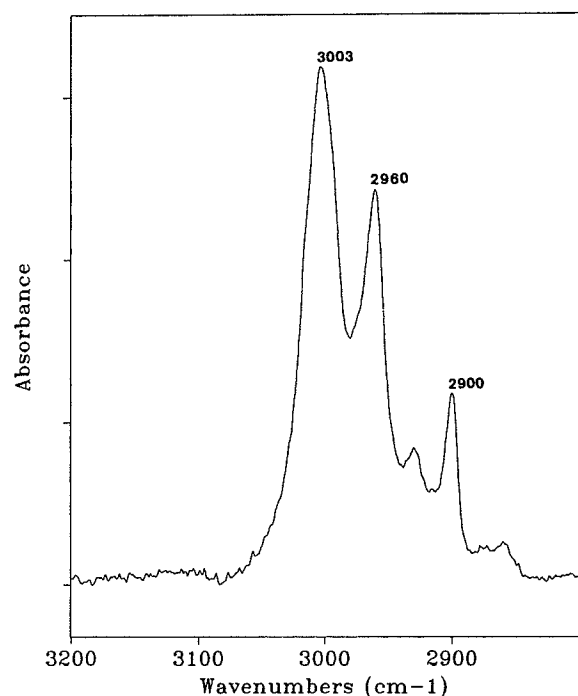
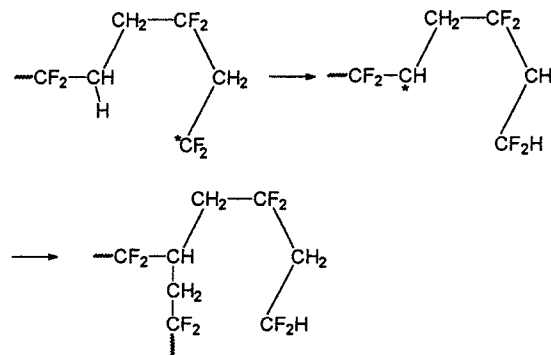


Fig. 8. IR spectrum (C–H stretching region) of a PFA sample (ethyl end groups).

hydrogen shift analogous to similar radical reactions reported in [22].

This reaction cannot occur in a normal chain, since the growing $-\text{CF}_2^*$ radical is always in a 1,4 or 1,6 relationship to $-\text{CH}_2-$ groups. Therefore, the 1,5 shift will come from 'head to head' sites, which are present at a concentration of about 3–5%, according to the following reaction:



This type of reaction then leads to some tertiary hydrogen sites in the polymer. In fact, the signal of a CH tertiary group (triplet, 77 ppm) has been observed by ^{13}C NMR spectroscopy. The $-\text{CH}_3$ end group can come from species formed in the same way by a growing radical ending with an inverted monomer unit, according to the following

Table 2
 ^{19}F NMR end groups assignments

Initiator/transfer agent	Assignment	^{19}F δ (ppm) vs. CFCl_3
$\text{BrCF}_2\text{CF}_2\text{Br}$	$-\text{CH}_2^{\text{B}}-\text{CF}_2^{\text{A}}-\text{CH}_2-\text{CF}_2^{\text{C}}\text{Br}$	-43.0 (A); -93.5 (B)
	$-\text{CF}_2-\text{CH}_2-\text{CH}_2-\text{CF}_2^{\text{D}}\text{Br}$	-45.0
	$-\text{CH}_2-\text{CF}_2-\text{CH}_2-\text{CF}_2^{\text{E}}-\text{CF}_2^{\text{F}}-\text{Br}$	-67 (E); -110.2 (F)
	$-\text{CH}_2-\text{CF}_2-\text{CH}_2-\text{CF}_2^{\text{G}}\text{H}$	-114.8 (G); -92.4 (H)
	$-\text{CF}_2-\text{CH}_2-\text{CH}_2-\text{CF}_2^{\text{I}}\text{H}$	-117.3
	$-\text{CH}_2^{\text{M}}-\text{CF}_2^{\text{L}}-\text{CF}_2-\text{CH}_3$	-107.8 (L); -114.3 (M)
PK 16 ^a	$-\text{O}-\text{CH}_2-\text{CF}_2^{\text{Q}}-\text{CH}_2-\text{CF}_2-$	-102.1
Di-benzoylperoxide	$\text{Ph}-\text{CH}_2-\text{CF}_2^{\text{R}}-\text{CH}_2-\text{CF}_2-$	-88.1
	$\text{Ph}-\text{COO}-\text{CH}_2-\text{CF}_2^{\text{R'}}-\text{CH}_2-\text{CF}_2-$	-101.1
Ammonium persulphate	$-\text{CF}_2^{\text{T}}-\text{CH}_2-\text{OH}$	-104.5
	$-\text{CF}_2^{\text{T'}}-\text{CH}_2-\text{OAc}$	-102.3
Ethyl acetate	$\text{CH}_3-\text{COO}-\text{CH}_2-\text{CH}_2-\text{CH}_2-\text{CF}_2^{\text{U}}-\text{CH}_2-$	-93.1
	$\text{CH}_3-\text{COO}-\text{CH}(\text{CH}_3)-\text{CH}_2-\text{CF}_2^{\text{V}}-\text{CH}_2-$	-93.1
Acetone	$\text{CH}_3-\text{CO}-\text{CH}_2-\text{CH}_2-\text{CF}_2^{\text{K}}-\text{CH}_2-\text{CF}_2-$	-94.3
Methyl acetate	$\text{CH}_3-\text{COO}-\text{CH}_2-\text{CH}_2-\text{CF}_2^{\text{Z}}-\text{CH}_2-\text{CF}_2-$	-93.1
CCl_4	$\text{CH}_2-\text{CF}_2-\text{CH}_2-\text{CF}_2^{\text{W}}-\text{CH}_2-\text{CF}_2\text{Cl}$	-47.6 (W); -93.1 (W')
	$\text{CH}_2-\text{CF}_2-\text{CF}_2-\text{CH}_2-\text{CH}_2-\text{CF}_2^{\text{X}}\text{Cl}$	-50.7
	$\text{CCl}_3-\text{CH}_2-\text{CF}_2^{\text{Y}}-\text{CH}_2-\text{CF}_2-\text{CH}_2-\text{CF}_2-$	-93.7

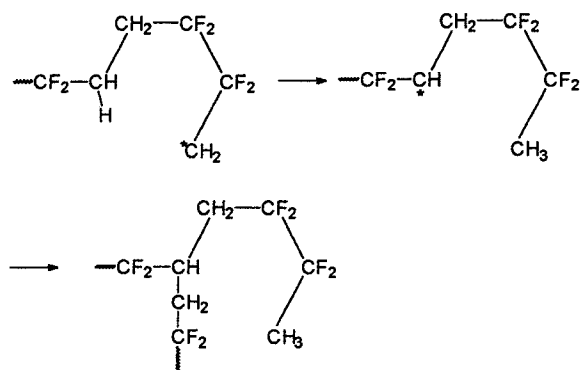
^a PK 16: bis(4-tertbutylcyclohexy)peroxy-dicarbonate.

Table 3
¹H NMR end groups assignments

Initiator/transfer agent	Assignment	¹ Hδ (ppm) vs. TMS
BrCF ₂ CF ₂ Br	—CH ₂ —CF ₂ —CH ₂ —CF ₂ Br ^A	3.5
	—CF ₂ —CH ₂ —CH ₂ —CF ₂ Br ^C	2.6
	—CF ₂ —CH ₂ —Br ^D	3.95
	—CH ₂ —CF ₂ —CH ₂ —CF ₂ H ^G	6.28
	—CF ₂ —CH ₂ —CH ₂ —CF ₂ H ^I	6.28
	—CH ₂ —CF ₂ —CF ₂ —CH ₃ ^L	1.78
PK 16 ^a	—C(CH ₃) ₃ ^N	0.85
	(CH ₃) ₃ C—(C ₆ H ₁₀)—O ^O —	1.0–2.2
	>CH—O ^P —	3.0
	—O—CH ₂ —CF ₂ —CH ₂ —CF ₂ — ^Q	4.5
Di-benzoylperoxide	Ph—CH ₂ —CF ₂ —CH ₂ —CF ₂ — ^R	2.5
	Ph—COO—CH ₂ —CF ₂ —CH ₂ —CF ₂ — ^{R'}	4.7
Di-tertbutylperoxide	CH ₃ —CH ₂ —CF ₂ — ^S	1.0
Ammonium persulphate	—CF ₂ —CH ₂ —OH ^T	3.9
	—CF ₂ —CH ₂ —OAc ^{T'}	4.3
Ethyl acetate	CH ₃ —COO—CH ₂ —CH ₂ —CH ₂ —CF ₂ —CH ₂ — ^{U'}	2.0 (U [*]); 4.2 (U ^{**})
	CH ₃ —COO—CH(CH ₃)—CH ₂ —CF ₂ —CH ₂ — ^{V'}	2 (V [*]); 5.2 (V ^{**}); 1.3 (V ^{***})
Acetone	CH ₃ —CO—CH ₂ —CH ₂ —CF ₂ — ^K	2.1
Methyl acetate	CH ₃ —COO—CH ₂ —CH ₂ —CF ₂ — ^Z	2.1
CCl ₄	CH ₂ —CF ₂ —CH ₂ —CF ₂ —CH ₂ —CF ₂ Cl ^{W''}	3.4
	CCl ₃ —CH ₂ —CF ₂ —CH ₂ —CF ₂ —CH ₂ —CF ₂ — ^Y	3.8

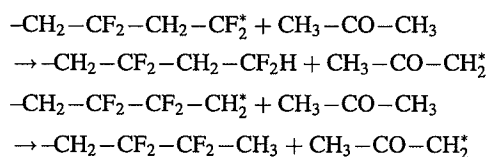
^a PK 16: bis(4-tertbutylcyclohexyl)peroxy-dicarbonate.

reaction:



—CH₂—CF₂H and —CF₂—CH₃ end groups have been observed also in [23], where is described the synthesis of low-molar-mass PVDF in three different solvents (acetone, ethyl acetate and methyl acetate). Here the solvent acts also as a chain transfer agent, by reacting with the growing macro-radical with a concurrent radical activity transferred to the solvent molecule by hydrogen abstraction.

With acetone we have the following reactions:



Reinitiation will give rise to the CH₃—CO—CH₂—CH₂—CF₂—CH₂—CF₂— end group. Tables 2 and 3 report ¹⁹F and ¹H NMR data related to such reinitiation end groups for the three solvents used.

As an example of COSY application, Fig. 9 shows the 282 MHz ¹⁹F two-dimensional correlated spectrum of a low molar mass PVDF synthesized in acetone. The sample has been dissolved in acetone-d₆ at 30°C and the spectra have been collected by an INOVA 300 spectrometer. A total of 64 transients has been accumulated for each of 512 spectra with 2048 points covering 10 000 Hz in both dimensions. The off diagonal or cross peaks observed indicate a connection between fluorine pairs which have scalar couplings, either through three or four bonds. The cross peaks marked by letters in the figure, concern only end groups and are

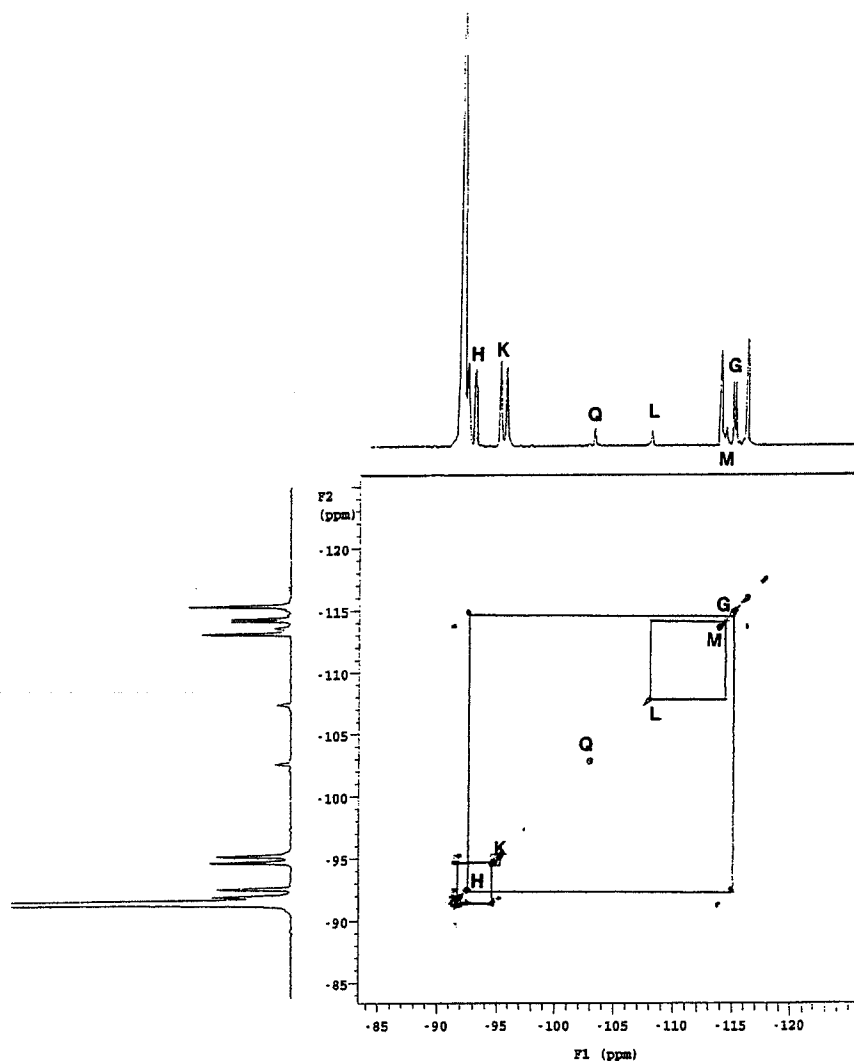


Fig. 9. 282 MHz ^{19}F 2D correlated NMR spectrum of a low molar mass PVDF synthesized in acetone. Attributions of the signals are reported in Table 2.

explained on the basis of the attributions reported in Table 2.

New end groups in VDF oligomers have been reported in [24], where it is demonstrated that the larger chain end groups ($-\text{Cl}$ and $-\text{CCl}_3$ as compared with $-\text{CH}_3$) tend to produce the conformational disorder in the molecules yielding the γ phase when the oligomers are crystallised from the melt. The new end groups were originated by CCl_4 present in the polymerisation system and were characterised by ^{19}F and ^{13}C NMR spectroscopy. In Fig. 10(A) and (B) are evidenced all the end groups observed on the ^{19}F and ^1H NMR spectra of a VDF oligomer obtained in conditions similar to those described in [24]. All assignments are reported in Tables 2 and 3.

End groups in VDF polymers at higher molecular weight (M_w about 90,000) have been studied by Madorskaya et al. [1]. They consider two types of PVDF, synthesised in an

aqueous medium either in the presence of potassium persulphate or of β -hydroxyethyl-*tert*-butyl-peroxide. The main difference between the two PVDF samples is in the structure of their end groups.

In persulphate polymerisation the end groups formed during initiation may be as follows:



End group (IV) gives HF and is almost instantaneously transformed into a carbonyl group ($-\text{CH}_2-\text{COF}$).

Hydrolysis of the ester group II takes place readily and leads ultimately to the formation of a terminal carbonyl ($-\text{CH}_2-\text{COF}$).

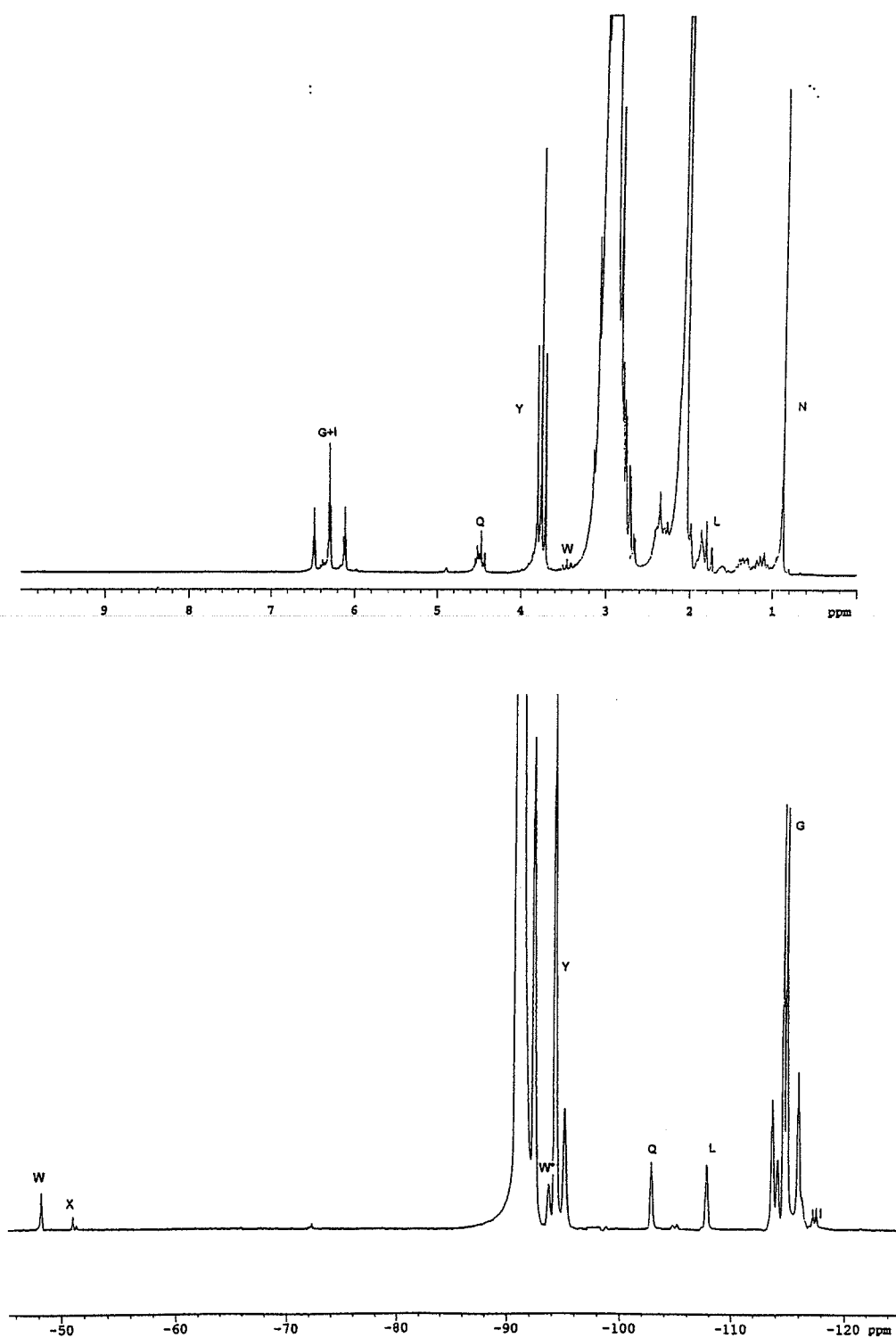


Fig. 10. (A) ^1H NMR spectrum of a low molar mass PVDF synthesized in CCl_4 . (B) ^{19}F NMR spectrum of the same sample. Attributions of the signals are reported in Tables 2 and 3.

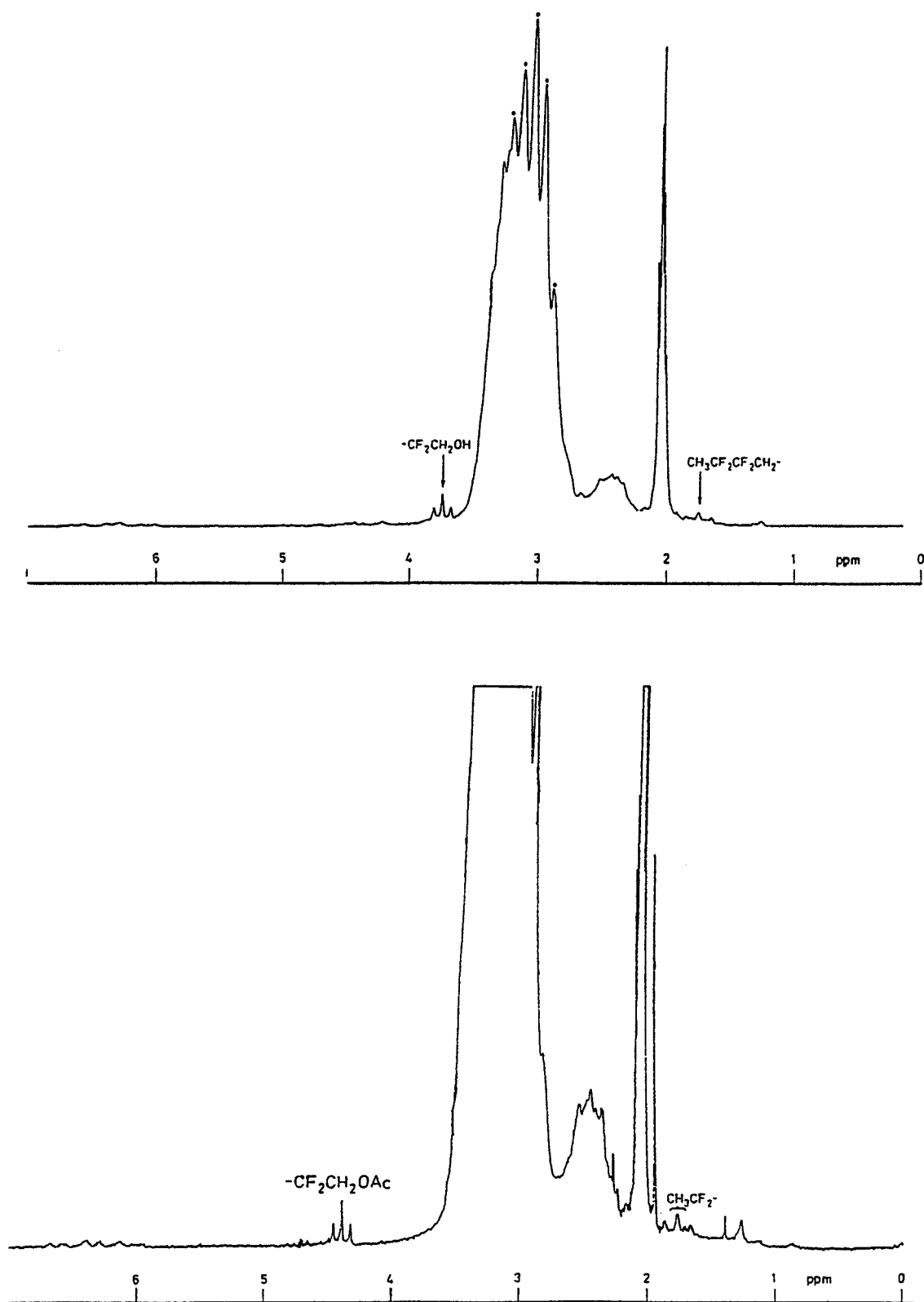


Fig. 11. ^1H NMR spectra of a high molar mass VDF-HFP copolymer before and after acetylation with acetic anhydride.

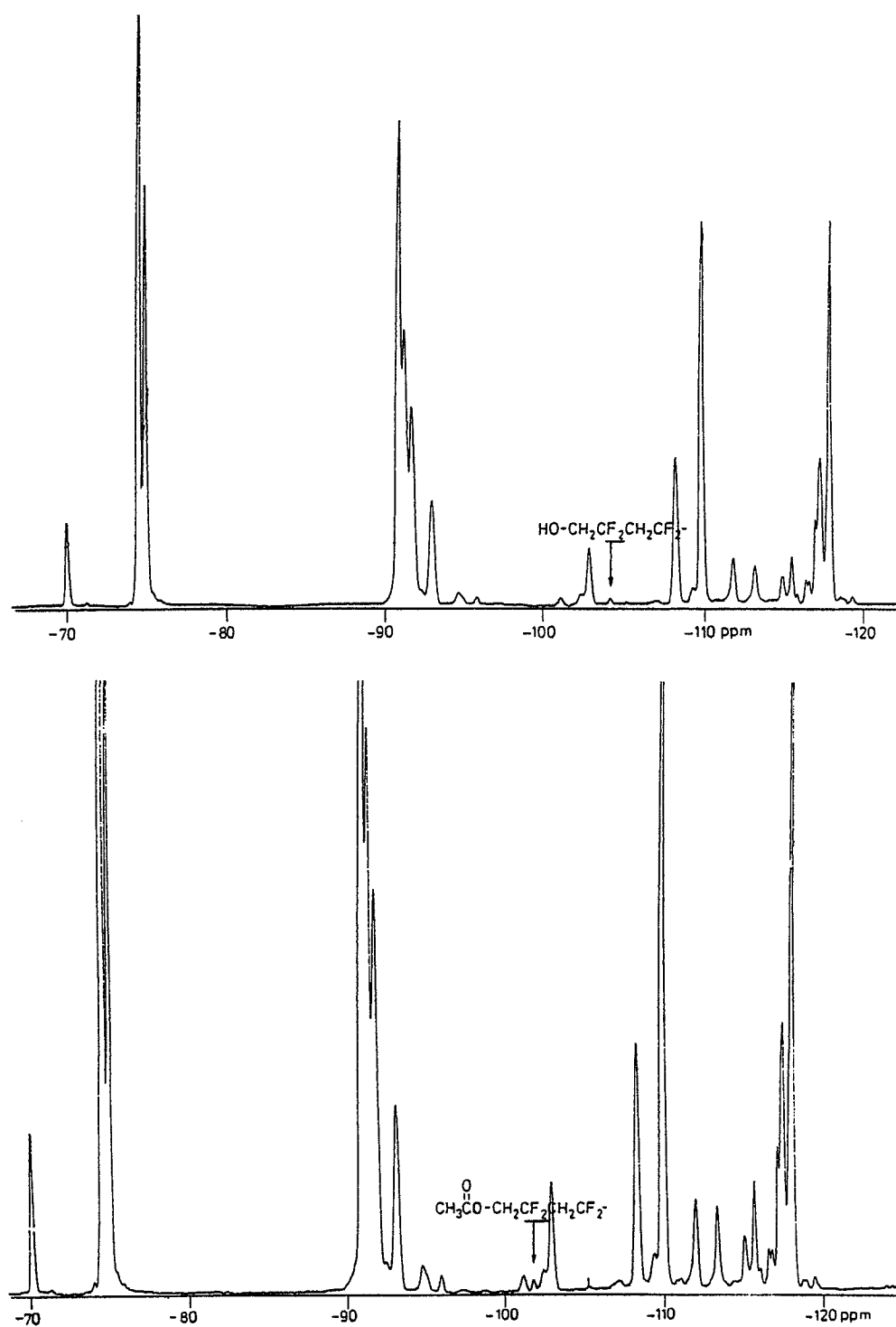


Fig. 12. ^{19}F NMR spectra of a high molar mass VDF–HFP copolymer before and after acetylation with acetic anhydride.

The ester bond in end group I is more stable than that in group II, but it is likewise subjected to hydrolysis giving a HO–CH₂–CF₂– terminal, as was evident from the appearance of an infrared band at 3550 cm⁻¹, related to an associated –OH group.

We have indeed always observed HO–CH₂–CF₂– end groups in samples of PVDF or of vinylidenefluoride/hexafluoropropene (VDF/HFP) copolymers synthesised in emulsion using ammonium persulphate as initiator. The related –CH₂– and –CF₂– NMR signals appear on their ¹H and ¹⁹F spectra, and the –OH group is observed as a band at 3636 cm⁻¹ in the IR spectrum. We have confirmed the assignments of Tables 2 and 3 by means of an acetylation reaction: the polymer is dissolved in acetic anhydride and is analysed after evaporation of the reaction mixture. ¹H and ¹⁹F NMR spectra show the expected shift of the signals due to the transformation of the alcohol to the acetic ester (Figs. 11 and 12), while the IR –OH band disappears and a new band appears at 1760 cm⁻¹ as expected from a CH₃–CO–O–CH₂–CF₂– group. In these polymers we could observe, by IR spectroscopy, a band at 1722 cm⁻¹ that is shifted to 1572 cm⁻¹ by exposition of the sample to ammonia vapours. Analogously to what observed in thermoplastic fluoropolymers, this behaviour is explained by the transformation of a –CF₂–CH₂–COOH carboxylic group into its ammonium salt.

The intensities of the 1722 cm⁻¹ (–C=O) and 3636 cm⁻¹ (–O–H) bands are of the same order of magnitude; considering the different absorption coefficients of the two groups, this means that hydroxyl end groups are about 10 times more abundant than carboxyls.

To investigate the structure of end groups in a VDF copolymer containing 5–7 mol% of TFE, Madorskaya [25] applied a radiotagging method. Using as initiator different samples of β-hydroxyethyl-*tert*-butyl peroxide labelled with ¹⁴C or ³H in various positions, it was possible to identify and quantify the following end groups:

- –CH₃ (63% of the total number of end groups);
- –CH₂–CF₂H (34%);
- (CH₃)₃C–O– (2%);
- HO–CH₂–CH₂–O– (1%).

By comparing the average number molecular mass of the VDF–TFE copolymer (equal to about 55 000 as determined by GPC analysis) with the total number of end groups, it was also proved the presence of branches, about 1.5 per 100 monomer units.

Comparing the proton NMR spectra of PVDFs obtained by persulphate or di-*tert*-butyl peroxide initiated polymerisation, we have observed that CH₃–CH₂–CF₂– is the only end group related to the di-*tert*-butyl peroxide initiator, due to the reaction of a methyl radical with a VDF molecule. It is easily observed in the proton NMR spectrum as a triplet at 1.05 ppm (Table 3).

–CH₂–CF₂H and –CF₂–CH₃ end groups are present in every commercial PVDF. Their NMR identification has

been described above and their formation can be attributed to chain transfer reactions induced by any hydrogen source in the polymerisation environment. The molar ratio –CH₂–CF₂H/–CF₂–CH₃ can vary between 1.2 and 4; the total content of the two end groups is strongly dependent on the polymerisation temperature and we have observed values ranging from 0.05 to 1 mole per 100 monomer units. Considering that in commercial PVDF the degree of polymerisation is in the range 800–1600, the high concentration of these end groups demonstrates the presence of branches.

4. Poly(vinylfluoride) (PVF)

¹⁹F NMR spectra of PVF are considerably more complicated than those of PVDF because two types of configurational disorder are possible: stereo-irregularity and regio-irregularity.

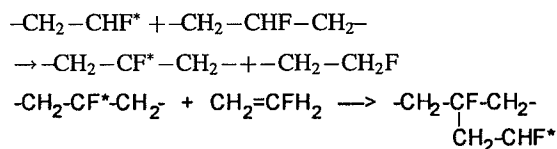
NMR and IR studies [26,27] have clearly established that PVF is largely stereo-irregular, irrespective of the polymerisation conditions used to prepare it, and detailed stereo-sequences assignments show that the polymer is predominantly atactic, with only a modest dominance of syndiotactic sequences.

The two main groups of peaks at about –180 and –190~–200 ppm in the ¹⁹F NMR spectra of PVF are due respectively to head to tail and head to head monomer sequences and their intensity ratio indicates that about 12–15% of the monomer units are reversed in commercial polymers.

In spite of their complexity, ¹⁹F NMR spectra of PVF give good information about end groups. As for PVDF, the more easily observable end groups are not originated by initiation or termination steps, but by an intra- or inter-molecular transfer of a hydrogen atom, leading to chain branching.

Weak peaks at –220 and –147 ppm, observed in the ¹⁹F NMR spectra run at 376.5 MHz of PVF samples swollen in Me₂SOd₆, have been attributed by Ovenal et al. [26] to –CH₂–CH₂F end groups and to tertiary fluorine atoms –CF< at branch points.

The –CH₂–CH₂F groups should arise from hydrogen abstraction by growing polymer radicals ending in –CHF*, according to the following mechanism, which results in the formation of tertiary fluorine atoms



The 400 MHz proton NMR spectrum of the same sample swollen in Me₂SOd₆ was too broad to directly identify weak peaks from branched structures, but by means of differential selective irradiation of the fluorine NMR spectrum at –220 ppm (corresponding to the weak –CH₂F resonances) a positive response from the –CH₂F protons was seen at

4.5 ppm and also a weaker response from the $-\text{CH}_2-\text{CH}_2\text{F}$ protons was observed at 2.0 ppm.

The correct interpretation of the weak signals in PVF ^{19}F NMR spectra allowed Aronson et al. [27] to associate the observed changes in the melting point of the polymer primarily with differences in the number of chain branch points, and not the regio-regularity.

References

- [1] L.Ya. Madorskaya, N.N. Loginova, Yu.A. Panshin, A.M. Lobanov, *Polym. Sci. USSR* 25 (1983) 2490.
- [2] J. Scheirs (Ed.), *Modern Fluoropolymers, High Performance Polymers for Diverse Applications*, Wiley, New York, 1997.
- [3] R.A. Morgan, W.H. Sloan, US Patent 4 626 587 (1986).
- [4] M.I. Bro, C.A. Sperati, *J. Polym. Sci.* 28 (1959) 289.
- [5] M.J. Pellerite, *J. Fluorine Chem.* 49 (1990) 43.
- [6] R.D. Lousenberg, M.S. Shoichet, *J. Org. Chem.* 62 (1997) 7844.
- [7] H.C. Gibbard, US Patent 5 180 803 (1993).
- [8] J.F. Imbalzano, D.L. Kerbow, US Patent 4 743 658 (1988).
- [9] M.D. Buckmaster, US Patent 5 093 409 (1992).
- [10] R.C. Schreyer, US Patent 3 085 083 (1963).
- [11] P. Colaianna, J.A. Abusleme, N. Del Fanti, US Patent 5 608 020 (1997).
- [12] P. Colaianna, J.A. Abusleme, N. Del Fanti, US Patent 5 618 897 (1997).
- [13] D.P. Carlson, European Patent Application 0 178 935 A1 (1985).
- [14] W.K. Fisher, J.C. Corelli, *J. Polym. Sci. Polym. Chem. Ed.* 19 (1981) 2465.
- [15] H. Vanni, J.F. Rabolt, *J. Polym. Sci. Polym. Phys. Ed.* 18 (1980) 587.
- [16] D. Fisher, U. Lappan, I. Hopfe, K.J. Eichhorn, K. Lunkwits, *Polymer* 39 (1998) 573.
- [17] H. Yu, J. Mi, H. Ni, *Chin. J. Microwave Radiofrequency Spectrosc.* 1 (1984) 372.
- [18] Ye.M. Murascheva, A.S. Shashkov, A.A. Dontsov, *Polym. Sci. USSR* 23 (1981) 711.
- [19] R.E. Cais, N.J.A. Sloane, *Polymer* 24 (1983) 179.
- [20] G. Luttringer, B. Meurer, G. Weill, *Polymer* 32 (1991) 884.
- [21] S. Modena, M. Pianca, M. Tatò, G. Moggi, S. Russo, *J. Fluorine Chem.* 43 (1989) 15.
- [22] W.C. Mattiew, F.C. Stehling, *Macromolecules* 14 (1981) 1479.
- [23] S. Russo, K. Behari, S. Chengji, M. Pianca, E. Barchiesi, G. Moggi, *Polymer* 34 (1993) 4777.
- [24] Herman, T. Uno, A. Kubono, S. Umemoto, T. Kikutani, N. Okui, *Polymer* 38 (1997) 1677.
- [25] L.Ya. Madorskaya, V.M. Samoilov, G.A. Otradina, A.P. Agapitov, V.P. Budtov, T.G. Makeyenko, Ye.Yu. Kharcheva, N.N. Loginova, *Polym. Sci. USSR* 26 (1984) 2891.
- [26] D.W. Ovenal, R.E. Uschold, *Macromolecules* 24 (1991) 3235.
- [27] M.T. Aronson, L.L. Berger, U.S. Honsberg, *Polymer* 34 (1993) 2546.